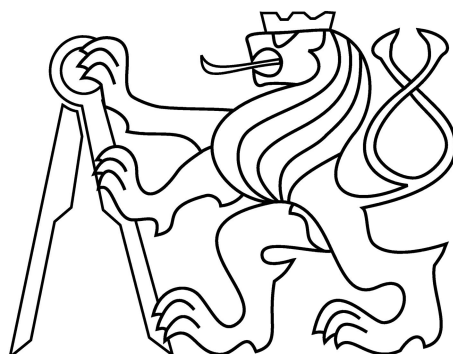


CZECH TECHNICAL UNIVERSITY IN PRAGUE  
FACULTY OF CIVIL ENGINEERING  
DEPARTMENT OF STEEL AND TIMBER STRUCTURES



# NUMERICAL ANALYSIS OF GLASS PANE: A blind point connection

---

Master's thesis

Bc. Jan Lorenz

Supervisor: Ing. Zdeněk Sokol, Ph.D.

Prague, December 2016



ČESKÉ VYSOKÉ UČENÍ TECHNICKÉ V PRAZE

Fakulta stavební  
Tháškova 7, 166 29 Praha 6

## ZADÁNÍ DIPLOMOVÉ PRÁCE

### I. OSOBNÍ A STUDIJNÍ ÚDAJE

Příjmení: Lorenz Jméno: Jan Osobní číslo: 396772  
Zadávací katedra: K134  
Studijní program: Civil Engineering  
Studijní obor: Building Structures

### II. ÚDAJE K DIPLOMOVÉ PRÁCI

Název diplomové práce: Numerická analýza kotvení skleněné tabule  
Název diplomové práce anglicky: Numerical analysis of glass pane

Pokyny pro vypracování:

Shrnutí problematiky kotvení skleněných konstrukcí, numerická analýza kotvení skleněné tabule pomocí skrytého bodu, parametrická studie, vypracování zásad pro návrh kotvení pomocí skrytého bodu.

Seznam doporučené literatury:

Jméno vedoucího diplomové práce: Zdeněk Sokol

Datum zadání diplomové práce: 6.10.2016

Termín odevzdání diplomové práce: 8.1.2016

Údaj uveďte v souladu s datem v časovém plánu příslušného ak. roku

  
Podpis vedoucího práce

  
Podpis vedoucího katedry

### III. PŘEVZETÍ ZADÁNÍ

*Beru na vědomí, že jsem povinen vypracovat diplomovou práci samostatně, bez cizí pomoci, s výjimkou poskytnutých konzultací. Seznam použité literatury, jiných pramenů a jmen konzultantů je nutné uvést v diplomové práci a při citování postupovat v souladu s metodickou příručkou ČVUT „Jak psát vysokoškolské závěrečné práce“ a metodickým pokynem ČVUT „O dodržování etických principů při přípravě vysokoškolských závěrečných prací“.*

13.10.2016  
Datum převzetí zadání

  
Podpis studenta(ky)

### Statutory declaration

I hereby declare that the master's thesis entitled "Numerical analysis of glass pane: A blind point connection" submitted to Czech Technical University in Prague was written by myself under the guidance of Ing. Zdeněk Sokol, Ph.D. I have stated all the resources used to elaborate this thesis in conformity with the Methodical guide for ethical development of university final thesis.

20<sup>th</sup> December 2016

Jan Lorenz

.....

## Aknowledgements

The work described in this thesis has been performed under the supervision of Ing. Zdeněk Sokol, Ph.D. at the Department of Steel and Timber Structures, Faculty of Civil Engineering, Czech Technical University in Prague. I would like to express my sincere gratitude to my supervisor for his personal guidance, patience and inspiring suggestions over the years of my studies as well as during the work on this thesis.

I would also like to give my thanks to doc. Ing Martina Eliášová, CSc for her encouraging help with both numerical modeling and experiments.

Also I would like to show my appreciation to the company OGB s.r.o. for providing me with samples from their production.

Last but not least, I would like to thank my family for their support and encouragement throughout the years.

## Abstract

Laminated glass is nowadays widely used construction material. It is not only because of its exceptional strength and reliability but also due to its appearance. The fact that we can use transparent building material opens up endless possibilities. But with design of laminated glass elements we also need to consider the design of connections to other parts of a structure. This can be a challenging task given the fact that there is still missing EC norm for glass structures which could guide us through the process of structural design. This leads to more or less trial-error experimental approach. The main aim of this thesis is to experiment with one of those connections, use FE software ANSYS Workbench to create a numerical model of that connection, confirm that the model corresponds to the reality, identify its characteristics and finally provide a parametric study of such connection with chosen parameter.

**Key words:** glass, laminated glass, glass-to-steel connections, point connections, blind point connection, numerical analysis, experimental analysis, delamination, cohesive zone modeling

## Contents

1. Introduction.....	11
2. Overview and state of the art .....	12
2.1. Glass in construction.....	12
2.2. Types of glass .....	13
2.2.1. Float glass.....	13
2.2.2. Tempered glass .....	14
2.2.3. Chemically strengthened glass.....	16
2.2.4. Laminated glass.....	17
2.3. Physical and material properties of glass .....	20
2.4. Glass structures connections .....	21
2.4.1. Glass load-bearing elements .....	22
2.4.2. Types of connections.....	24
3. The aim of diploma thesis .....	33
4. Experimental analysis.....	33
4.1. Description of experiments .....	33
4.2. Tested specimens.....	37
4.2.1. F1-01.....	38
4.2.2. F1-02.....	39
4.2.3. F1-03.....	40
4.3. Testing equipment .....	41
4.3.1. MTS QTest 100 .....	41
4.3.2. EIR Laser Extensometer.....	42
4.3.3. Steel Load Frame.....	42
4.3.4. Steel Bed.....	43
4.4. Testing procedure .....	43
4.5. Test results .....	43
4.5.1. F1-01.....	44
4.5.2. F1-02.....	46
4.5.3. F1-03.....	50
4.5.4. Evaluation of experiments .....	52

4.5.5.	Conclusion .....	54
5.	Numerical analysis.....	55
5.1.	Numerical model.....	55
5.1.1.	General conditions .....	55
5.1.2.	Model geometry.....	58
5.1.3.	The meshed model.....	60
5.1.4.	Material properties .....	62
5.1.5.	Calculation procedure .....	64
5.2.	Results.....	65
5.3.	Parametric study.....	68
5.3.1.	Description .....	68
5.3.2.	Results .....	69
6.	Conclusion .....	70
6.1.	Summary .....	71
6.2.	Future extensions .....	72
7.	Bibliography .....	73

## Figure index

Figure 2.1 Greenhouse at Chatsworth, UK, 1840 [1] .....	13
Figure 2.2 Float glass process [11].....	14
Figure 2.3 Stress distribution in fully tempered glass cross-section [10].....	15
Figure 2.4 Comparison of the thermally and chemically strengthened glass [10].....	17
Figure 2.5 Laminated glass scheme [5] .....	17
Figure 2.6 Behavior of glass panes subjected to bending [4].....	18
Figure 2.7 Approximation curve showing the relationship between shear modulus G and temperature T (laminated safety glass) [4] .....	20
Figure 2.8 Overview of connection types [10] .....	22
Figure 2.9 Large deflection theory vs. small deflection theory [10] .....	23
Figure 2.10 The cross-section of glass-concrete beam and the specimen during test [12].....	24
Figure 2.11 Types of support [10] .....	25
Figure 2.12 Standard bolt connection - shear bolt [10] .....	26
Figure 2.13 Countersunk-head bolt connection [10] .....	26
Figure 2.14 Bolted connection with steel splices [10].....	27
Figure 2.15 Bearing bolt connection with splices [10] .....	28
Figure 2.16 Friction bolt connection with splices [10] .....	28
Figure 2.17 Bolted connection with stud assembly [10].....	29
Figure 2.18 Spider connection [10] .....	30
Figure 2.19 Spider - adhesive point fixing [10].....	30
Figure 2.20 Articulated bolt connection [10] .....	31
Figure 2.21 Different adhesives' behavior [10] .....	32
Figure 4.1 Cross-section and top view of a sample.....	34
Figure 4.2 Detail of a blind connection fitting.....	34
Figure 4.3 Experiment scheme .....	35
Figure 4.4 A load frame and a sample set up inside of load frame.....	35
Figure 4.5 Glass failure .....	36
Figure 4.6 Delamination .....	36
Figure 4.7 Interlayer foil failure.....	37
Figure 4.8 F1-01 sample .....	37
Figure 4.9 The non-uniform thickness of a liner .....	38
Figure 4.10 Bubbles around the connection fitting (F1-01) .....	39
Figure 4.11 Bubbles around the connection fitting (F1-02) .....	39
Figure 4.12 The non-uniform thickness of the liner and group of bubbles (F1-03).....	40
Figure 4.13 Surface scratch (F1-03).....	40
Figure 4.14 MTS QTest 100.....	41
Figure 4.15 The laser extensometer (left) and magnets with reflective tape (right).....	42
Figure 4.16 The sketch of the load frame (left) and the manufactured load frame (right).....	42
Figure 4.17 A steel bed with cylindrical supports and plastic washers.....	43

Figure 4.18 Delamination of connection fitting (F1-01).....	44
Figure 4.19 Spreading delamination and brittle failure (F1-01).....	45
Figure 4.20 Ripped out connection fitting (F1-01).....	45
Figure 4.21 Foil-fitting delamination, note the change of color of the liner due to vacuum inside (F1-02).....	48
Figure 4.22 Origin and the propagation of glass-foil delamination.....	49
Figure 4.23 Destroyed heat-strengthened glass pane with the connection fitting imprint, float glass pane is intact (F1-02).....	49
Figure 4.24 Foil-fitting delamination (F1-03).....	51
Figure 4.25 Glass-foil delamination (F1-03).....	51
Figure 4.26 Destroyed heat-strengthened glass pane with the connection fitting imprint, float glass pane is intact (F1-03).....	52
Figure 5.1 FE model boundary conditions.....	56
Figure 5.2 Separation-distance based debonding.....	56
Figure 5.3 Delamination – contact stress.....	57
Figure 5.4 FEA delamination.....	58
Figure 5.5 Scheme of the model (experiment - thin line, model - thick line).....	58
Figure 5.6 Geometry of the model.....	59
Figure 5.7 Model - detail of the connection fitting.....	59
Figure 5.8 SOLID185 finite element [15].....	60
Figure 5.9 SOLID186 finite element [15].....	60
Figure 5.10 CONTA174 finite element [15].....	61
Figure 5.11 TARGE170 finite element [15].....	61
Figure 5.12 The meshed model.....	62
Figure 5.13 ANSYS static structural.....	65
Figure 5.14 Deformation of the model.....	66
Figure 5.15 Gap opening on the connection fitting - interlayer foil interface.....	66
Figure 5.16 Dimensions of different connection fittings.....	68
Figure 6.1 Scheme of the performed work.....	71

## Table Index

Table 1 Material properties of glass [5] .....	21
Table 2 Values obtained from the experiment data .....	53
Table 3 Material properties of glass (FEA x typical) .....	62
Table 4 Material properties of HDPE (FEA x typical) .....	63
Table 5 Material properties of stainless steel (FEA x typical) .....	63
Table 6 Material properties of SentryGlass (FEA x typical) .....	64
Table 7 FE model x ideal blind point connection .....	67

## Graph Index

Graph 1 Force - deflection diagram (F1-01) .....	46
Graph 2 Force - deflection diagram (F1-02) .....	47
Graph 3 Force - time diagram (F1-02) .....	47
Graph 4 Force - deflection diagram (F1-03) .....	50
Graph 5 Force - time diagram (F1-03) .....	50
Graph 6 Force-deflection diagram of all samples .....	53
Graph 7 Force-deflection diagram of ideal blind point connection .....	54
Graph 8 Force-deflection graph of pre-delamination behavior .....	67
Graph 9 Stiffnesses of different connection fittings .....	69
Graph 10 Delamination force-diameter dependency .....	70

## 1. Introduction

For the past few decades as well as nowadays there have been countless buildings reflecting the modern trends in architecture and in construction industry in general. Use of large transparent areas has become a standard for both commercial and non-commercial buildings. The material which allows building these modern structures in such a way is glass, a material unique for its optical and mechanical properties. Unlike common structural materials such as concrete and steel, glass does not have the ability to reach plastic deformation. It behaves elastically until brittle failure. This means that while designing a glass element, we cannot consider reduction of stress peaks due to plastification or redistribution of loading stresses like we do for example with steel. This fact leads to necessity of careful design of the element itself as well as all the connections.

The glass load bearing structures which do not only support their own weight but also live load, snow load and wind load are nowadays widely used as facades, footbridges, balustrades or even roof structures. Some other applications such as glass beams or columns show that glass as a building material is very appealing. Despite all of this, we still have quite limited information about glass as a structural material. For a design of a structural glass element, the designer is usually left with insufficient know-how and regulations and is forced to gain the needed knowledge by an experimental way. It should be said that those difficulties are redeemed by properties of structural glass such as transparency, high compressive strength, corrosion resistance and many others.

The aim of this work is to help designers with use of blind point connection by providing its typical characteristics validated by both experimental and numerical analysis.

## 2. Overview and state of the art

### 2.1. Glass in construction

It is well documented that glass has been used by mankind for millennia. Not only for fashion and art purposes but also as a filling material to enclose space. It is one of the oldest manmade building material and at the same time a material which is mostly perceived as a very modern one [1]. It influences our lives probably more than we think. The biggest and most unique advantage of this material is its transparency. Given this fact it is no wonder that glass is very popular among both architects and civil engineers. On the other hand we must say that it has also indisputable disadvantage in the form of its brittleness. The broken glass pane has a zero load bearing capacity and it must be designed in such way that it does not come to that.

The modern history of glass structures starts in the early 19<sup>th</sup> century in England. The desire for growing exotic plants forces gardeners and engineers to start building greenhouses and experiment with new building materials of glass and iron. They know that for greenhouses to work properly there must be significantly more glass than iron in the structure and it forces them for the first time in history to use glass as a load bearing material usually in a form of folded plate or a dome structure [1]. From the look at some of those greenhouses it can be seen that it is not only functional design but also a very aesthetically pleasing one.

Nowadays we use glass everywhere, from construction of bus stops to the highest skyscrapers. Thanks to countless researchers we have many types of glass usable in almost every thinkable situation. Glass that varies in optical, physical or mechanical properties, is soundproof, withstands being hit by a hammer or even bulletproof. This with wide variety of possible connection components really makes glass not only a modern building material but also a building material of the future.

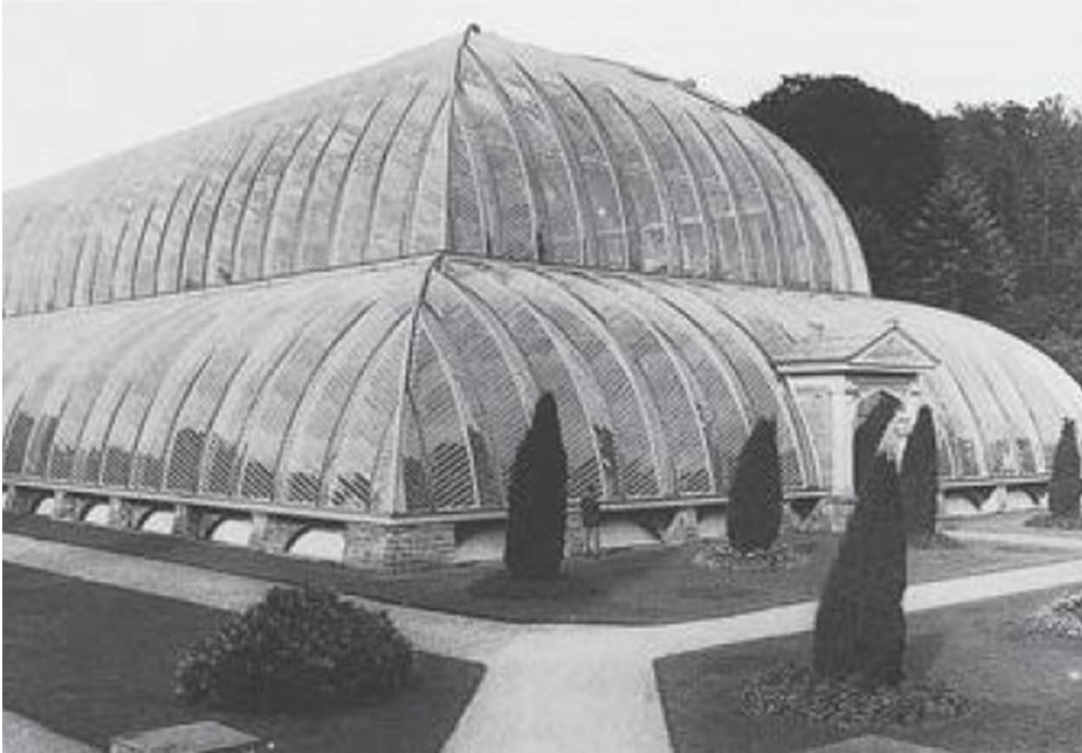


*Figure 2.1 Greenhouse at Chatsworth, UK, 1840 [1]*

## 2.2. Types of glass

We can organize glass into many categories according to many different properties. In the civil engineering we usually organize it according to process of manufacture. Then the types of glass are:

- Float glass
- Tempered glass
- Chemically strengthened glass
- Laminated glass

### 2.2.1. Float glass

Float glass is nowadays made by so called float glass process (also known as Pilkington process) introduced in 1952 by Sir Alastair Pilkington in the UK. It is manufactured from mixture of raw materials and cullet (recycled glass). The main chemical ingredients for the

float glass process are silica sand, soda ash, limestone and sodium sulfate. These materials are mixed together with recycled glass and then heated in a furnace up to 1500 °C. The molten glass is then cooled down to around 1000 °C and continuously fed onto the top of tin bath. The molten glass floats on tin and creates a glass “ribbon” with uniform thickness. The desired thickness of the (slowly solidifying) ribbon can be regulated by the stretching effect of the conveyers [6, 11]. Glass slowly cools down in an annealing lehr and is then further processed. The width of the ribbon is adjusted to be uniform and then it is cut into glass panes. Typical thicknesses available from producers are 3, 4, 5, 6, 7, 8, 10, 12, 15, 19 and 25 mm. The maximum dimensions of a pane are 6,0 x 3,2 m. The dimensional accuracy ranges around  $\pm 2 - 4$  mm for length and squareness and  $\pm 0,2 - 1,0$  mm for thickness (the amount depends on nominal thickness) [10].

Despite its brittle behavior and relatively low tensile strength (around 40 MPa) the flat glass is still being used in construction business in applications where those are not limiting factors. When broken it shatters into big sharp fragments.

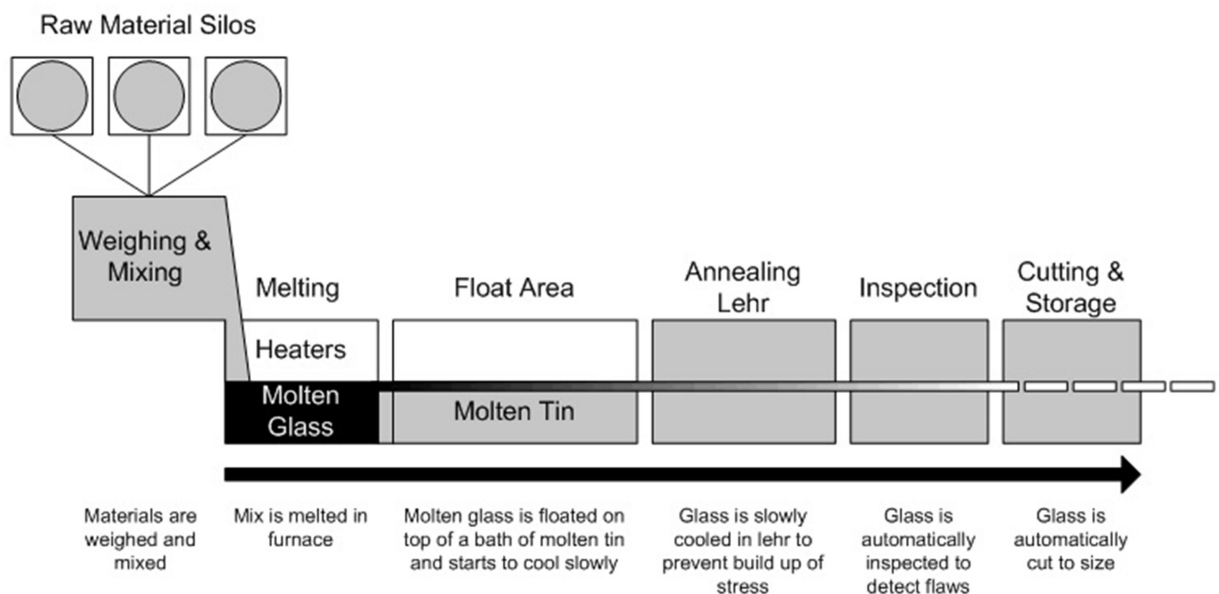


Figure 2.2 Float glass process [11]

### 2.2.2. Tempered glass

Some situations require such mechanical properties of a material which flat glass just cannot satisfy. For those applications there are ways how to improve its resistance to

mechanical and thermal loads. Tempered glass is one of those improvements. We can divide tempered glass into two categories:

- Fully tempered glass
- Partially tempered glass

**Fully tempered glass** (or toughened glass) is made by a heat treatment of float glass. Float glass panes are heated up to 650 °C and then suddenly cooled down. As a cooling process happens very quickly, it causes the surface of a glass pane to shrink more rapidly than the core. This basically means that the pane is prestressed. The compressed surface is in equilibrium with the core which is in tension [10]. The stress distribution is of a parabolic shape (fig 2.3)

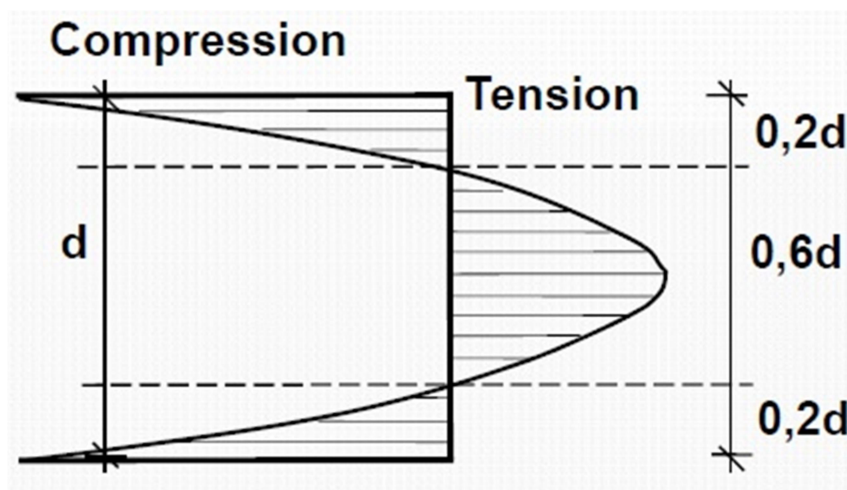


Figure 2.3 Stress distribution in fully tempered glass cross-section [10]

Thanks to this process such glass has a high value of bending strength as a result of high compressive surface stress (up to 150 MPa) combined with tensile strength of float glass. There are few other things on the plus side of this product. Toughened glass withstands local temperature differences up to 150 °C (float glass only 40 °C) and when broken it shatters into small pieces thus it is not as dangerous situation as it would be with float glass. The main disadvantage of toughened glass is possible spontaneous fracture. It usually happens up to two years after production and is caused by nickel

sulphide volume expansion [6]. Also all mechanical work as cutting or drilling must be done before the heat treatment since afterwards it is not possible. Another disadvantage is greater initial deformation of glass panes caused by transport rollers during the heat treatment. The initial deformation has a sinusoidal shape and a value up to  $L/300$ . For the comparison the maximal initial deformation of float glass is  $L/2500$  [10].

**Partially tempered glass** (or heat-strengthened glass) is produced in a similar manner as toughened glass. It is heated up to same temperature of  $650\text{ }^{\circ}\text{C}$  and then cooled down but the cooling process is slower so the surface prestress is not so great. The internal stress ranges from 35 to 55 MPa and it withstands local temperature differences up to  $100\text{ }^{\circ}\text{C}$ . Unlike toughened glass this type of glass does not have problem with spontaneous fracture due to nickel sulphide inclusions [6]. When broken the fragmentation is very similar to float glass fracture [7]. It can be seen from its properties that this type of glass is pretty much a compromise between float glass and toughened glass.

### 2.2.3. Chemically strengthened glass

It is another type of strength refined glass. The difference from the tempered glass is that the prestress here is caused by an ionic exchange. It is made by dipping a glass pane into electrolytic bath where sodium ions are replaced by potassium ions. Potassium ions are bit bigger than sodium ones so this exchange causes surface compression. The fracture behavior of such pane is similar to float glass. This type of strengthened glass can be cut or drilled in even after the treatment. The edges then have the strength of float glass. The other big advantage is absence of thermal deformation, which makes this glass perfect material for manufacturing of very thin glass panes. On the other hand such glass is very susceptible to surface defects due to small thickness of strengthened zone [10].

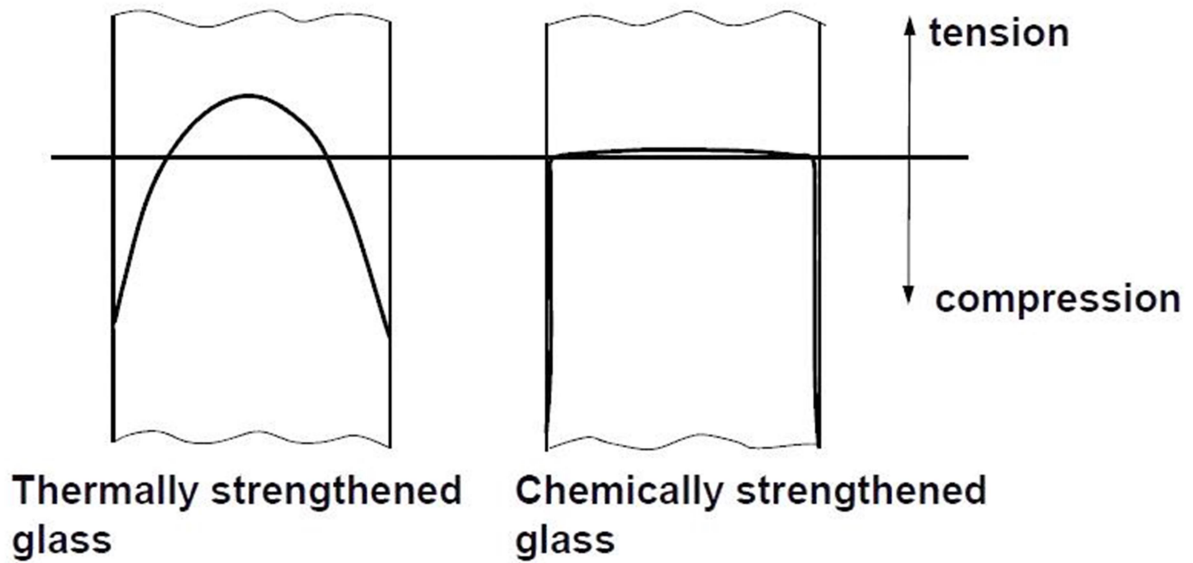


Figure 2.4 Comparison of the thermally and chemically strengthened glass [10]

#### 2.2.4. Laminated glass

Laminated glass is a type of glass invented in France in the beginning of 20<sup>th</sup> century by Edouard Benedictus [5]. It consists of multiple glass panes (float or strength refined ones) connected to each other. The connection is provided by a polymeric foil or in some cases by a resin lamination. This composition has a huge positive impact on properties such as load-bearing capacity, robustness or safety. Due to these improvements such glass can be used for roof structures, load bearing elements (columns, beams), windscreens or even as a bulletproof glass.

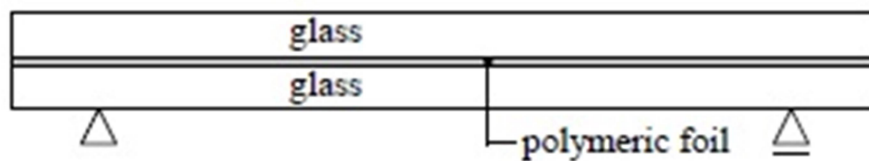


Figure 2.5 Laminated glass scheme [5]

During the manufacturing process, desired number of glass panes and foils are layered and positioned. This assembly is then preheated up to 70 °C and pressed

(prelaminated) by a calender. The air in between panes and foils is squeezed out. Then the prelaminated product is heated in an autoclave up to 140 °C and laminated under pressure around 800 kPa. Other way of lamination process uses resin interlayer (epoxy, acrylic, polyester) instead of polymeric foil. In that case glass panes are vertically positioned next to each other with requested gap in between them which is then filled by liquid resin. Such panes can be made in bigger sizes since the manufacture is not limited by size of an autoclave [10].

Laminated glass can have some significant advantages over monolithic glass panes. The characteristics of laminated glass strongly depends on type of glass, its thickness and number of panes as well as on the type of interlayer used, its thickness and quantity of sheets used. The main possible advantages ones are described below.

**Composite behavior:** The laminated glass is made of two different materials – glass and polymeric interlayer. This influences both full and residual load-bearing capacity. The interlayer is too thin to have reasonable flexural stiffness but it is able to provide shear stress in between the glass panes thus increasing the stiffness and load-bearing capacity of the laminated pane [4]. This is illustrated in the figure 2.6 together with borderline cases (layered limit –  $G = 0$  and monolithic limit –  $G = \infty$ )

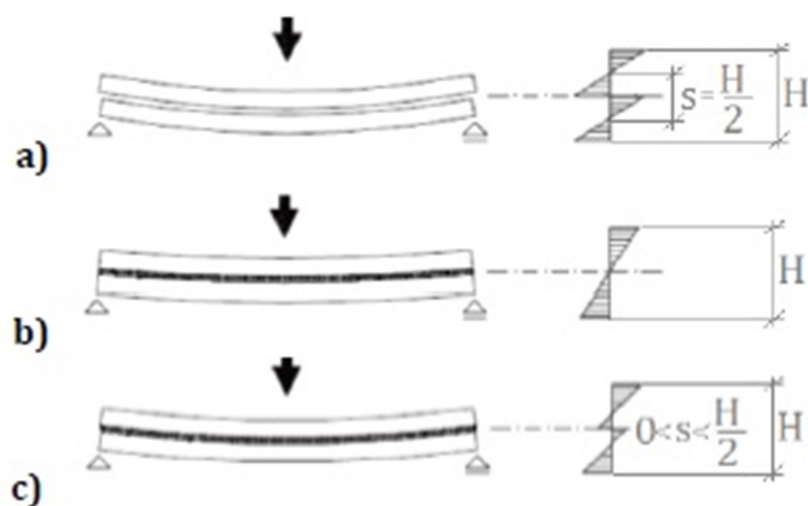


Figure 2.6 Behavior of glass panes subjected to bending [4]

a) layered behavior

b) monolithic behavior (stiff interlayer)

c) composite behavior (flexible interlayer)

**Safety:** When broken to pieces, fragments remain bonded to the foil preventing the complete collapse of a member. Glazing is still in its place and thanks to its residual load-bearing capacity it further protects the interior environment of a building until it is replaced for a new one. This applies to numerous situations such as harsh climatic conditions (strong wind, hurricane ...), forced break-in or vandalism.

**Heat gains control:** This is something that needs to be carefully considered when designing large glazed areas. The appropriate glazing system can help to manage interior temperature by the amount of solar energy transferred through. This can be achieved by a combination of a suitable interlayer with proper glass type. It should be designed accordingly to the type of climate the building is in.

**Sound insulation:** Laminated glass provides an excellent sound reduction. Thanks to viscoelastic behavior of an interlayer the laminated glass has serious sound reducing qualities over the monolithic glass of the same thickness. This is particularly true for PVB foil and cast-in-place resin. Such glass can be successfully used as an effective partition wall in modern office spaces.

**UV control:** Specialized interlayers can also reduce effect of UV radiation by absorbing all light wavelengths except the visible range. This ensures that there is enough light in the interior but the curtains, carpet and overall furnishings stay intact from the damaging effects of the UV radiation [4, 5].

The behavior of laminated glass also depends of course in the used interlayer. The interlayer keeps the glass bonded to itself even when broken and has other important functions as mentioned before. There is a wide range of different interlayers and each of them has different qualities. The most common types of interlayers are listed below:

- PVB (polyvinyl butyral)
- EVA (ethylene-vinyl acetate)
- PE (polyethylene)
- IP (ionoplast)
- PU (polyurethane)

- Cast-in-place resin

Each interlayer affects the mechanical behavior of laminated glass under the load in different way. The cause of that is difference in the shear modulus  $G$  of each type of interlayer. The example of such difference can be seen on the figure 2.6. There is obvious change in stress redistribution when  $G = 0$  (figure 2.6a),  $G = \infty$  (figure 2.6b) and  $0 < G < \infty$  (figure 2.6c). As the interlayers are made of viscoelastic materials it must be said that shear modulus  $G$  changes with temperature and duration of load [4, 10]. This can be clearly seen in the figure 2.7

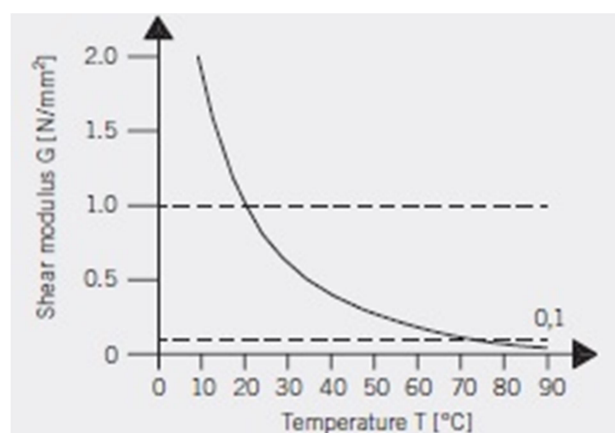


Figure 2.7 Approximation curve showing the relationship between shear modulus  $G$  and temperature  $T$  (laminated safety glass) [4]

### 2.3. Physical and material properties of glass

Glass is a very different material in comparison with common building materials. It has many unique features which will be described in this chapter. Glass is an amorphous (non-crystalline) material with viscoelastic behavior. It is solid at room temperature but turns liquid above the transition temperature ( $\sim 580$  °C). Soda-lime glass is a most common type of float glass, typically used in construction business. It is a durable transparent material which is resistant to water, salt water, corrosion, organic solvents and even strong acids. Glass behaves elastically until brittle failure [10]. That is due to high content of silicone dioxide ( $\text{SiO}_2$ ) which highly influences both strength of glass as well as its fragility. The compressive strength of glass is comparable with the compressive strength of high performance steel. On the other hand its tensile strength is not so

impressive although its value is still bigger than tensile strength of concrete or timber. The tensile strength of glass could be theoretically in thousands of MPa in case of the perfect microstructure and flawless surface but the real tensile strength is greatly influenced by micro and macro cracks which randomly occurs on the surface of glass. These imperfections originate in manufacture process or are caused by further manipulation with glass such as cutting drilling or even cleaning. The strength of glass also depends on the size of an element, the duration of load action and air humidity [6]. The most important material properties of float glass are summarized in the following table.

Property	Value	Unit
Density	2,520	kg.m <sup>-3</sup>
Tensile strength	20 – 100	MPa
Compressive strength	400 – 900	MPa
Modulus of elasticity	70 – 74	GPa
Shear modulus	20 – 30	GPa
Poisson's ratio	0.22 – 0.25	-
Thermal expansion factor	$8 \times 10^{-6} - 9 \times 10^{-6}$	K <sup>-1</sup>

Table 1 Material properties of glass [5]

## 2.4. Glass structures connections

When designing a structure, connections in between different load-bearing elements are very important part of the construction. The same also applies for glass structures but as was stated earlier, due to elastic behavior of glass until its brittle failure the connections here are really crucial section of the design. Typically we use glass-to-steel connections, primarily used for glazed façade systems or glass balustrades but glass-to-glass connections are also possible. Those can be needed when creating for example a glass frame. When designing such connections one must always remember the nature of mechanical properties of glass – elastic, until brittle failure, and make the connections accordingly. That means that development of local stress peaks and stress concentration needs to be avoided as well as direct contact in between glass and metal fittings [6]. This is usually solved by a separating layer made of plastic, resin or polyamide. Connections of

load-bearing glass elements can be designed as point, linear or mixed supports (figure 2.8).

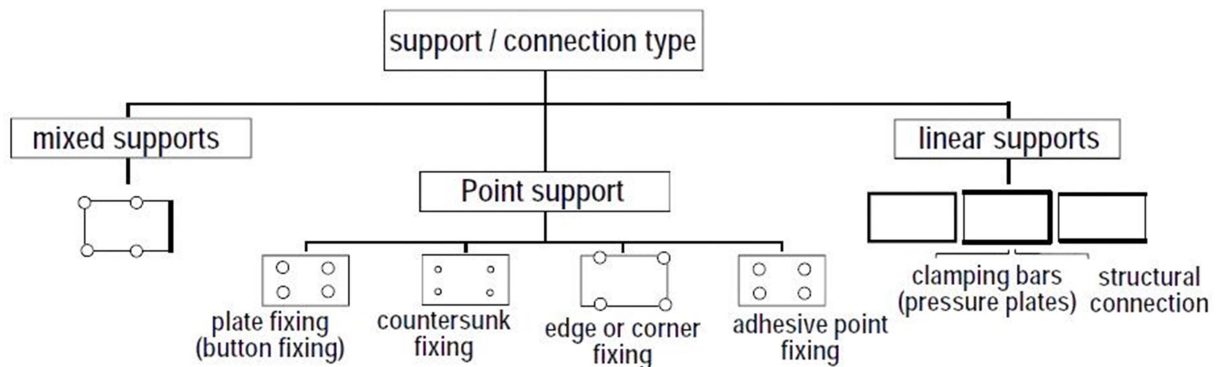


Figure 2.8 Overview of connection types [10]

### 2.4.1. Glass load-bearing elements

#### Compression members

Although it is not common, glass bars can be used as a compression member in a truss. The example of such structure can be found in restaurant Amstelveen in Netherlands where 30 mm glass bars together with steel profiles form a hybrid truss beams. The other application for glass compression members is to form glass columns. As those would seem very appealing as glass columns should, they are not so widely used. The reason for that is mostly lack of information and knowledge about glass members subjected to combination of normal force and bending moments [6]. Nevertheless there are examples of glass columns loaded axially. The example of such column was developed by Brunet & Saunier and was successfully used in St. Germain-en-Laye municipal building in 1994. Its cross-section has shape of a regular cross, it is made from 3-layer laminated glass and has height 3,2 meters. Maximum loading was calculated to be 69 kN [10].

#### Glass panes

Panes are nowadays the most used load-bearing members made of glass. They are used in construction of glazed facades, footbridges, roofs, balustrades or stairs. They are members subjected to bending and their structural behavior is strongly influenced by the type of connection to the supporting structure. For plates with deflection bigger than

their thickness, large deflection theory (influence of membrane stress) should be used otherwise the design will not be economic [6, 10] (figure 2.9).

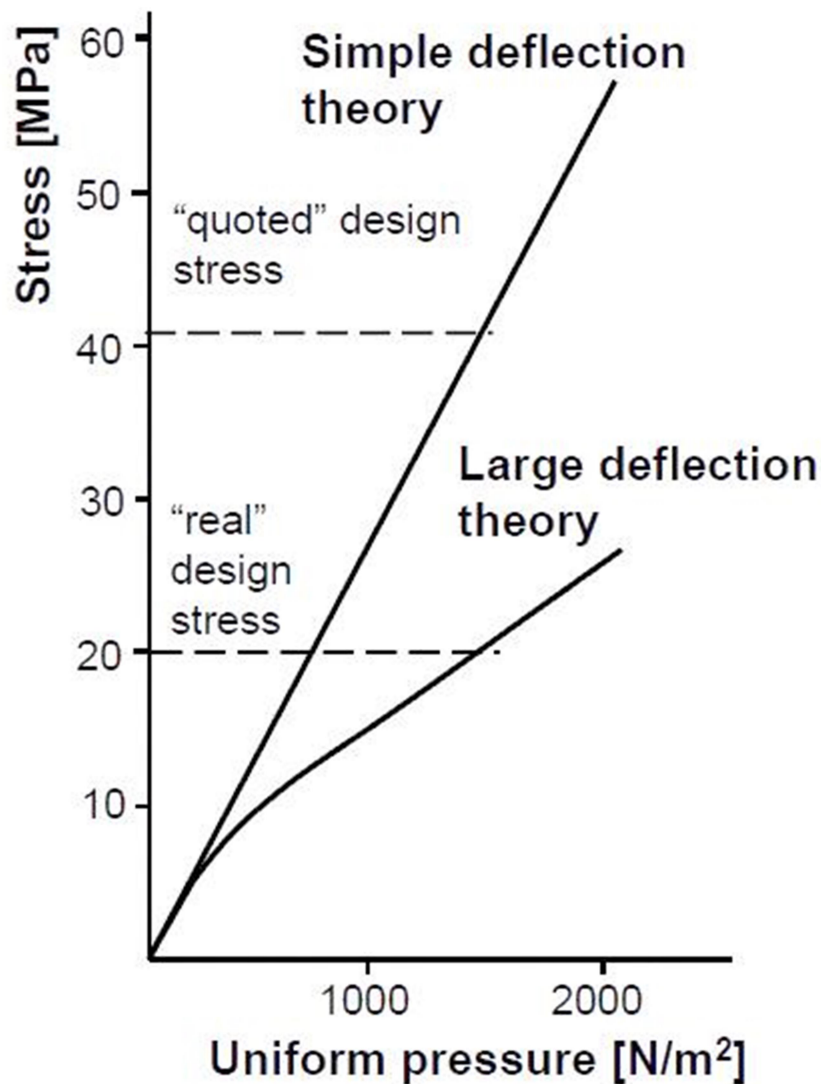


Figure 2.9 Large deflection theory vs. small deflection theory [10]

## Beams

Beams are horizontal elements subjected to loading by bending moment around their strong axis. The bearing capacity of glass beams is limited by lateral torsional and local buckling and tensile bending stresses. They are used as simply supported or cantilevering. Maximum length of glass beams is around 6 meters [10]. Sometimes the glass is combined with other material to form a hybrid beam. Other materials such as timber, concrete or steel create flange while glass forms a web of a beam.



Figure 2.10 The cross-section of glass-concrete beam and the specimen during test [12]

### Glass fins

Fins are vertical or sloping elements used for supporting of glazed facades. They have been used since 1950s to stiffen shop windows. They are oriented perpendicularly to façade, thus acting as vertical beam transferring the wind load [1]. As beams they are loaded by bending moment. They are made either as simple supported or fully cantilevering. Fins longer than 8 meters are usually top-hang, shorter ones are bottom supported. The type of connection between a fin and a glazed façade determines the structural behavior of the fin. Adhesive or bolted connections are used in such situation [6].

#### 2.4.2. Types of connections

Whether the structure is constructed purely out of glass members or is connected to supporting structure there is always need for connections in between structural members. Such connections are usually designed as bolted ones. Bolted connections are easy to produce, to visually inspect and to repair. On the other hand architect might require clean looks of the connections, not interrupted by steel bolts. For such situations glued connections seem like the best solution. Apart from type of attachment we can also categorize connections according to their type of support. Such division is shown in figure 2.11.

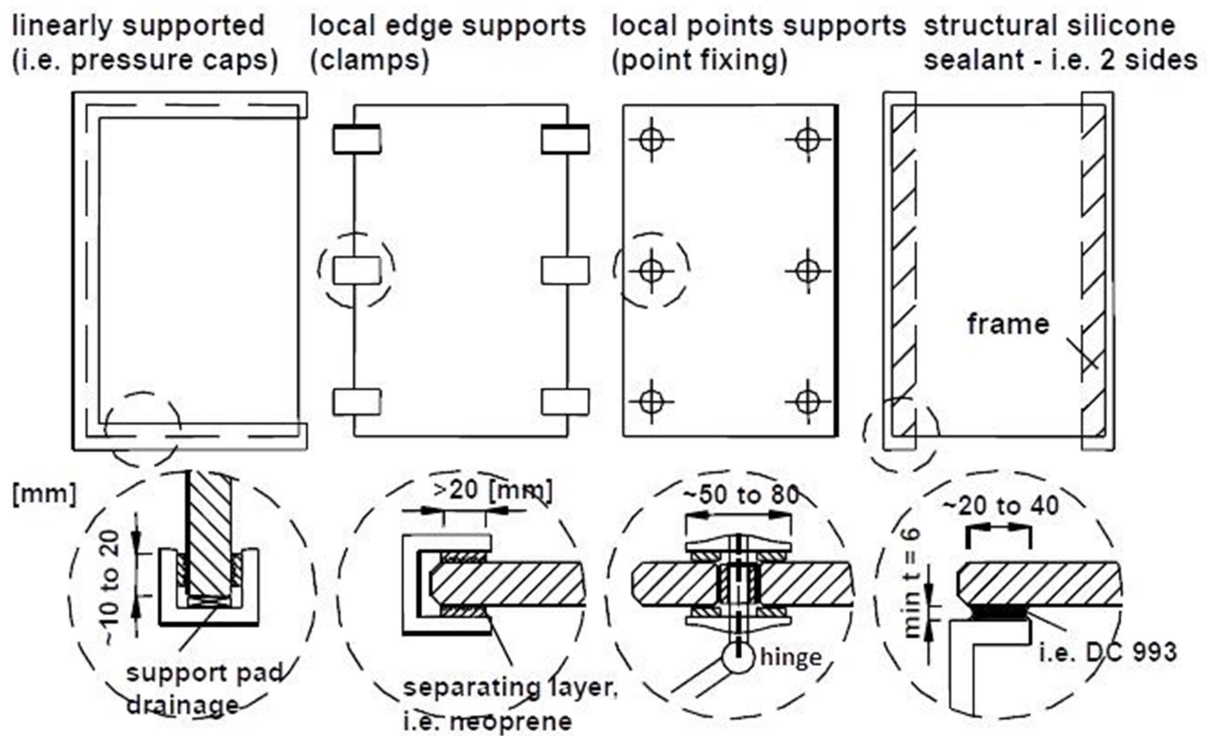


Figure 2.11 Types of support [10]

There are more detailed descriptions of important types of connections in the following text.

#### Standard bolt connection – shear bolt

This connection is the simplest type of fixing glass load-bearing members. Typical bolts are used here so their heads stick out of the glass plane. The load action from the glass pane is transferred by bearing on the shank of the bolt. The contact area is very small (even if there is a liner used) so the resistance of this connection is not so big in comparison with the other types of connections. Also since the glass is firmly fixed to the supporting structure, there is very little capacity for rotation if under out-of plane load. Due to these limiting factors there are big local stress peaks in the glass around the bolt [6].

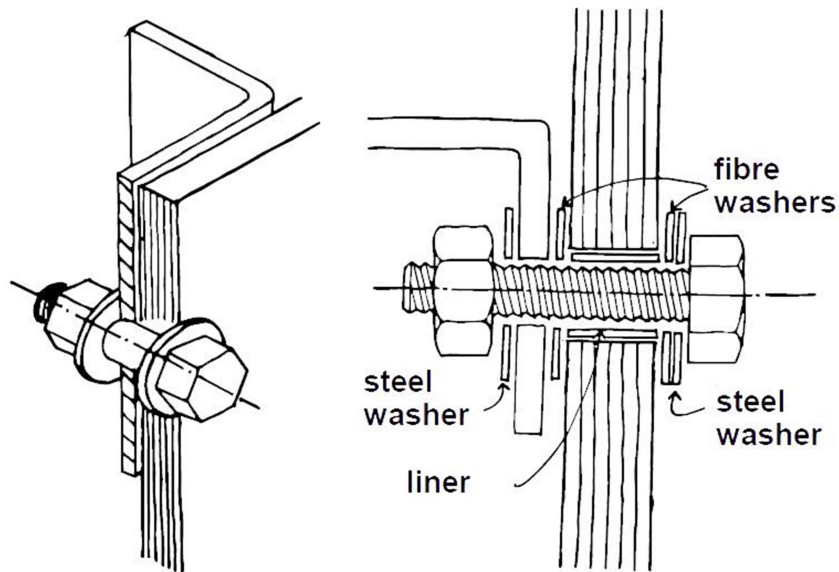


Figure 2.12 Standard bolt connection - shear bolt [10]

#### Simple countersunk-head bolt

This type of connection is very similar to the previous one. The biggest difference is in the bolt head which is leveled with a glass plane. This improves the in-plane load capacity due to enhanced contact area yet due to limited rotation during the out-of plane loads there is still possibility of failure due to big local stress peaks in glass around the bolt [10].

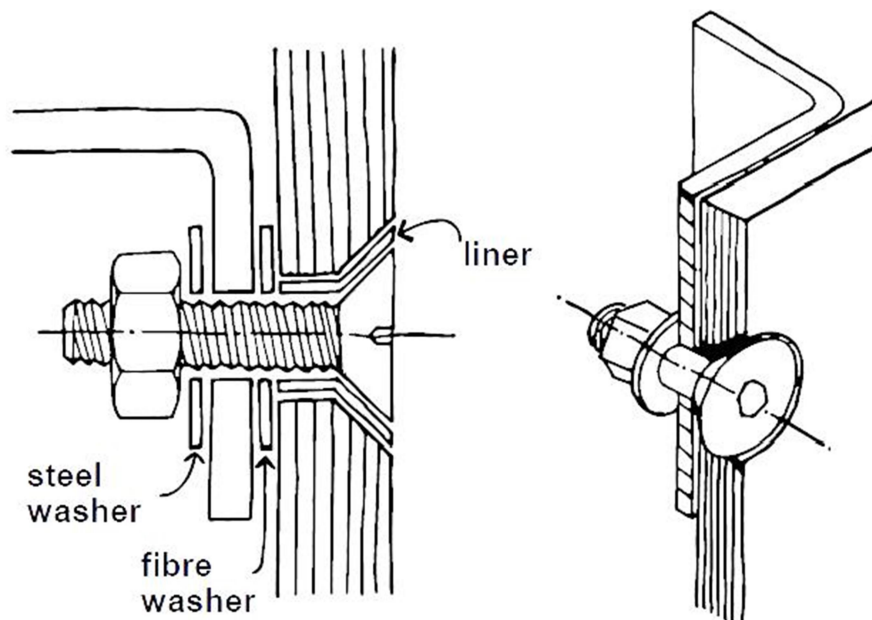


Figure 2.13 Countersunk-head bolt connection [10]

### Bolted connection with steel splices

This is usually realized as double shear or friction connection with steel splices at both sides of the glass pane. Depending on the type of this connection bearing bolts or friction bolts can be used.

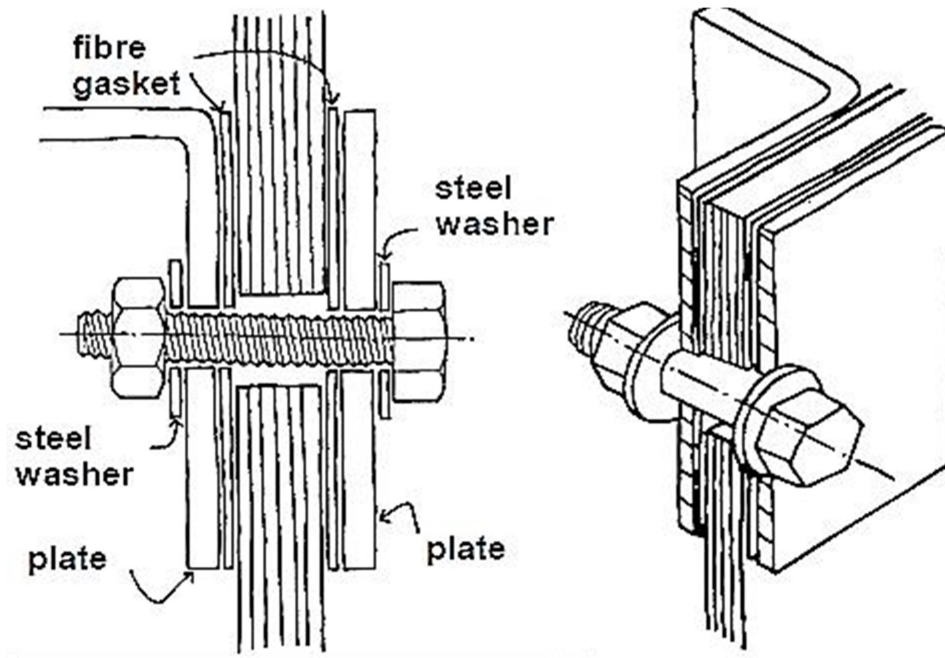


Figure 2.14 Bolted connection with steel splices [10]

- Bearing bolts with steel splices

Type of connection which is suitable only for tempered or heat strengthened glass due to big stress concentration around bolt holes. Loads are transferred directly from glass plane through contact in between a suitable interlayer and bolt bearing surface. The load-bearing capacity of such connection depends on the number of bolts used and their diameter. To avoid eccentricity in the connection, there are usually two splices used [10]. The scheme and behavior of such connection is illustrated in figure 2.15.

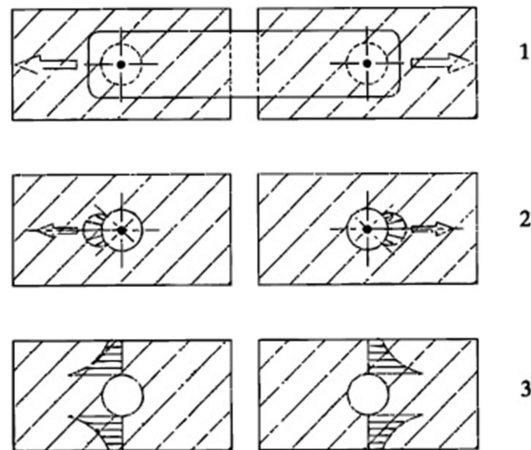


Figure 2.15 Bearing bolt connection with splices [10]

- 1) Scheme of the connection
- 2) Compressive stress in the glass pane
- 3) Tensile stress in the glass pane

- Friction bolts with steel splices

Such connection is realized by use of friction bolts. Bolt holes can be bigger than usually because transfer of loads is provided by friction contact between glass panes and steel splices. Due to this feature, this type of connection enables rectification of a glass pane during construction. Friction layer is added to the surface of steel splices to enhance the load-bearing capacity of this connection. This layer also protects glass from the direct contact with steel. To ensure the functionality of this connection, bolts have to be prestressed. Special torque wrench must be used to prestress bolts to the predefined force [9].

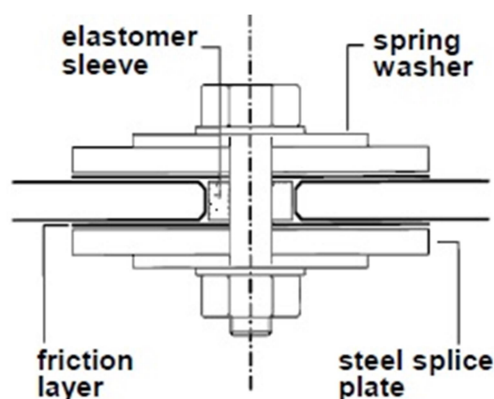


Figure 2.16 Friction bolt connection with splices [10]

### Bolted connection with stud assembly

A type of connection realized with multiple bolts, a stud and a backplate. It is characterized by high in-plane load-bearing capacity. Countersunk bolts are typically used here to provide a smooth surface of a connection. Bolt holes are made bigger than bolts since they are not supposed to carry vertical loading. That is ensured by a stud with bigger contact area. Bolts carry only out-of plane loads. Such connection does not have a provision for rotation of a glass pane under the influence of out-of plane loading. The disadvantage of this connection is a necessity of drilling of multiple bolt holes close to each other [6, 10].

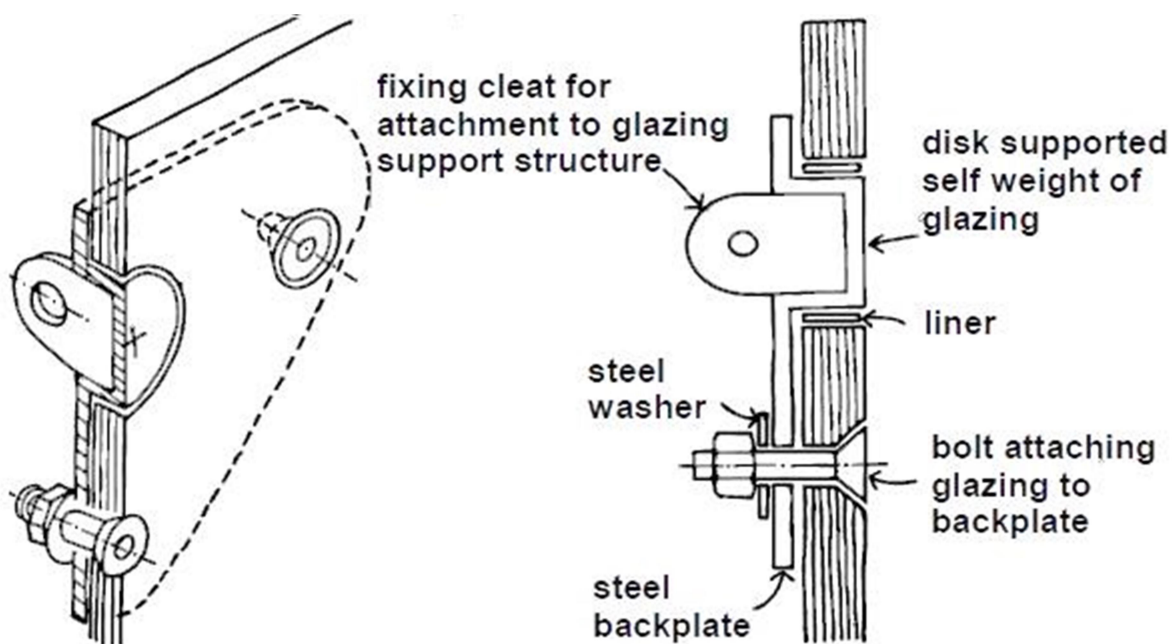


Figure 2.17 Bolted connection with stud assembly [10]

### Spider connection

This is a widely used type of point connection. Typically it uses countersunk-head bolts usually installed with predetermined torque. The spider can have one, two, three or four cantilevering arms supported in its center. The big advantage of this connection is use of flexible washers in both bolt hole and brackets (from neoprene for example) allowing the bolt to rotate relatively to arms. Such construction minimizes a bending moment transferred by a glass pane [1, 10].

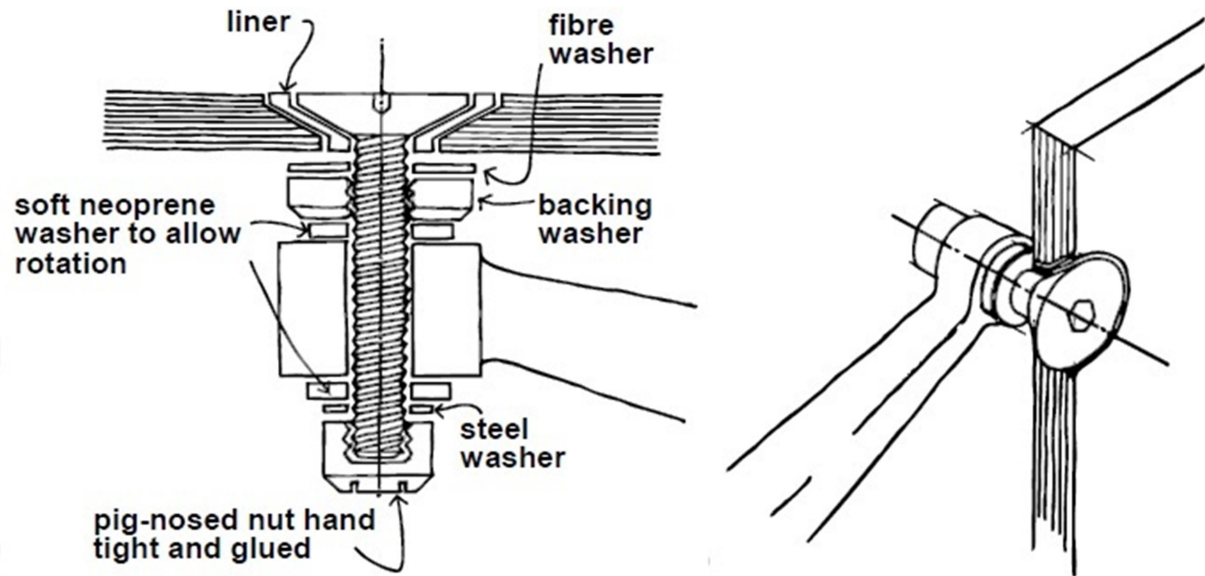


Figure 2.18 Spider connection [10]

Spider connection can be successfully used also with other types of joining than with countersunk-head bolts. The bolts can be replaced by adhesive point fixing or with a special undercut hole fitting (blind point connection). Such fitting is hidden inside of laminated glass and is especially suitable for applications where the clean look uninterrupted by visible connections is required.

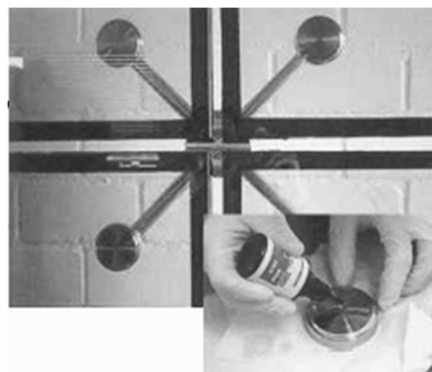


Figure 2.19 Spider - adhesive point fixing [10]

### Articulated bolt connection

Such connection uses bolts with spherical bearing surfaces instead of standard bolt heads. The bolt holes are adjusted to be fitted by a bearing cup matching a spherical bolt head. Such bolts are designed to be able to allow bigger rotational movement of the glass pane

relative to the supporting structure. Due to this quality this connection acts as a hinge thus is not transferring bending moments into the glass pane [6].

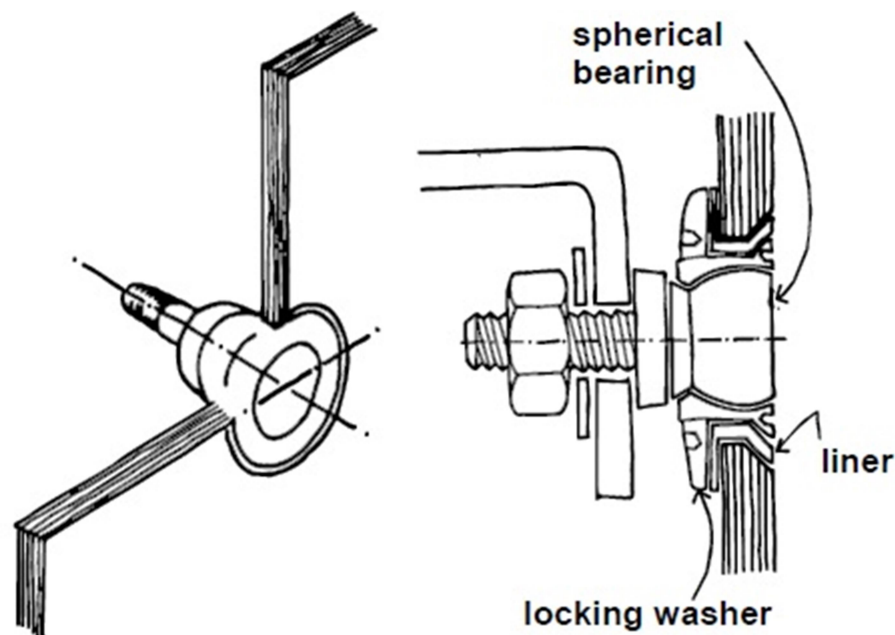


Figure 2.20 Articulated bolt connection [10]

### Glued connections

Unlike steel which is well-researched and well predictable material, glass is an elastic brittle material which has still not been well-researched for the structural use. The adhesive bonding is a modern joining technique connecting two different materials while trying to benefit from advantages of such hybrid connection. In such connection both materials should be used in a way which is ideal according to their material properties. This approach is used for example in automotive or ship building industry with great success but in civil engineering it is still mostly used for bonding of structures with non-significant structural importance. Still glued connections offer some advantages compared to conventional joining types [3, 10]. These are the major advantages:

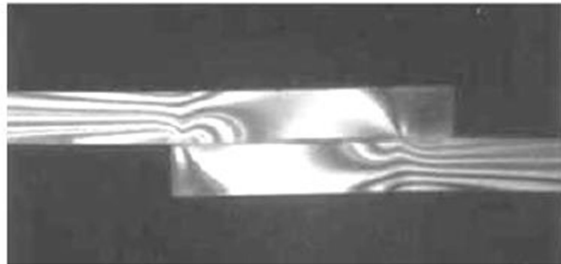
- No weakening of cross section by drilling holes
- Reduction in weight
- Aesthetic improvement
- Better stress distribution
- Joining acts also as sealing

- Vibration damping
- Compensation of tolerances

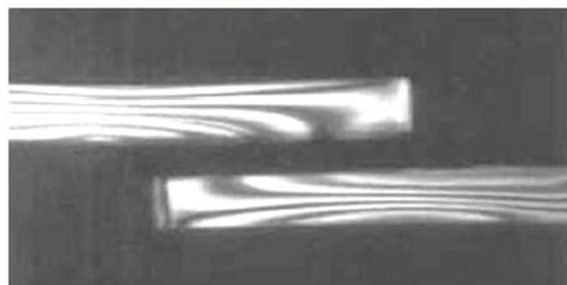
On the other hand glued connections are influenced by ageing, temperature, humidity and UV radiation. Compared to the conventional connections they have limited fire-resistance and their long-time behavior is affected by creeping. The glass surface must be of course prepared for application of a glued connection.

It should be also said that the behavior of adhesive bonding strongly depends on type of adhesive and the thickness of the adhesive layer. The following are the mostly used adhesives:

- Cyanoacrylates
- Modified epoxies
- Polyurethane resin
- Structural silicones



**Stress peaks in the ends of a lapped connection formed with a hard adhesive**



**Uniform distribution of stress in connection formed with a thick elastic adhesive**

*Figure 2.21 Different adhesives' behavior [10]*

### 3. The aim of diploma thesis

There were numerous possible types of connections used in glass structures construction described in the previous chapter. Design of such connections is necessary to verify by experiments since there still is missing both theoretical and practical knowledge for such design. To conduct those experiments is both money and time demanding.

The aim of this thesis is to determine basic characteristics needed for design of blind point connection mentioned in the spider connection paragraph in the previous chapter. This connection is very modern type of joining technique therefore there are no guidelines or regulations for its design.

To determine the behavior and characteristics of this connection, two methods will be used:

- Experimental analysis
- Numerical analysis

Also a parametric study will be performed to find out how different input parameters influence the behavior of this type of point connection.

## 4. Experimental analysis

### 4.1. Description of experiments

The experiments were performed on three samples. Their dimensions are 500mm x 300 mm. Each sample consists of 10 mm float glass, 4 layers of SentryGlass foil (0,38 mm each), 10 mm heat-strengthened glass and stainless steel blind connection with HDPE liners (figure 4.1). The blind connection consists of a stainless steel fitting laminated into the SentryGlass foil. The fitting is enclosed in by a heat-strengthened glass pane and secured by a stainless nut from the outside (figure 4.2). The nut should be tightened to the prescribed torque moment (10 Nm).

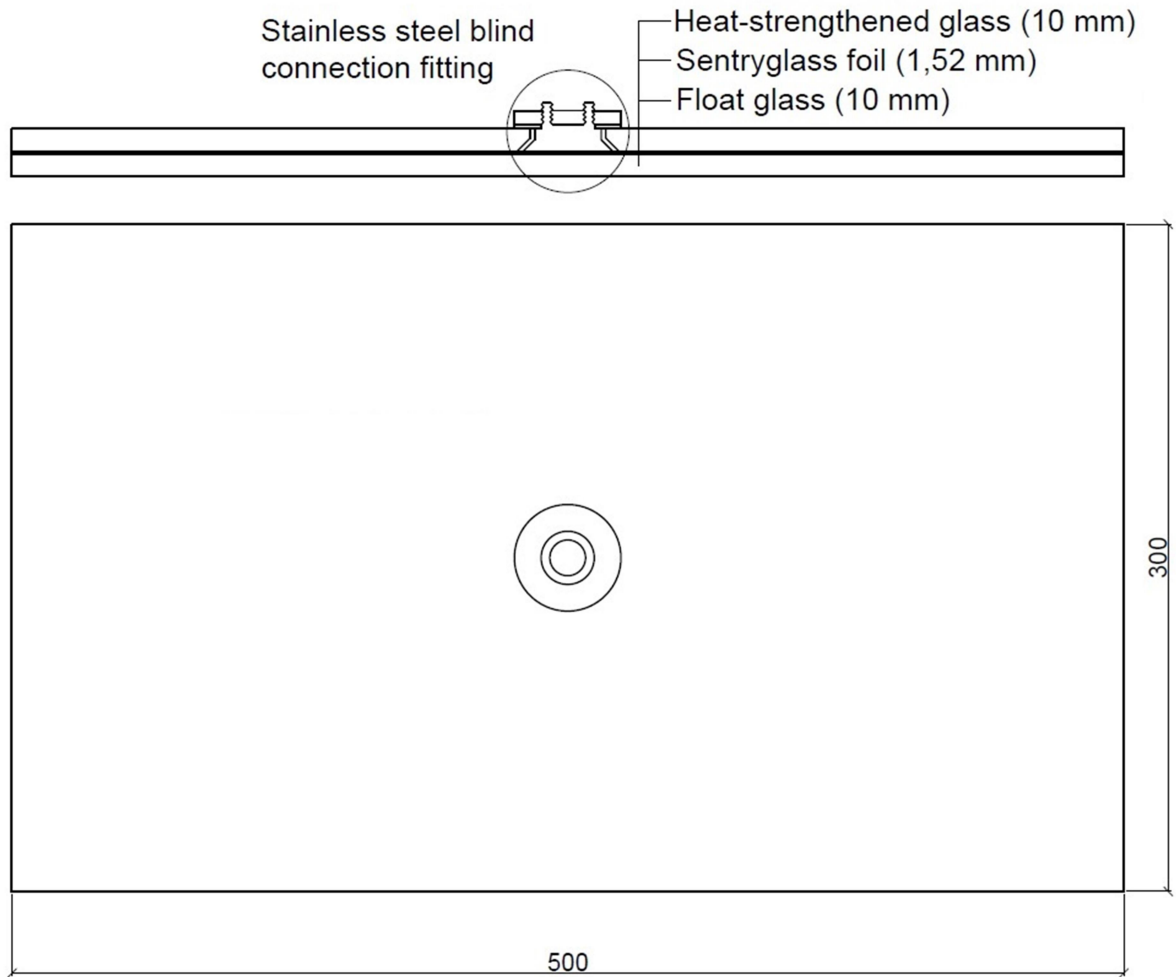


Figure 4.1 Cross-section and top view of a sample



Figure 4.2 Detail of a blind connection fitting

Samples were tested for a tensional load-bearing resistance. The panes were supported by two cylindrical supports as a simply supported beam. There were also plastic washers on both steel cylindrical supports to avoid crushing of the glass in contact places. The scheme of this setup is depicted in figure 4.3.

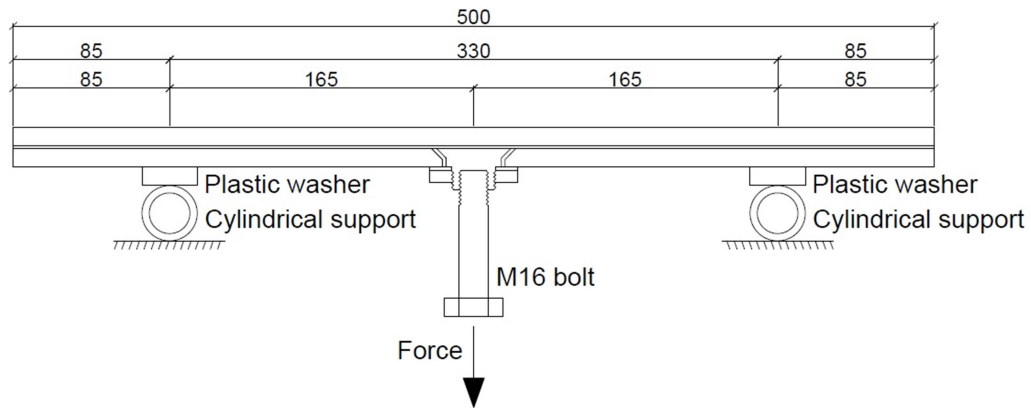


Figure 4.3 Experiment scheme

A special load frame had to be manufactured to apply the load such as is depicted in figure 4.3. It was welded together from 60x60x4 SHS profiles and 5 mm steel sheet with detachable bottom part. The frame can be seen in figure 4.4.



Figure 4.4 A load frame and a sample set up inside of load frame

There were several failure modes expected to occur during the testing:

#### Glass failure

A brittle failure of weakened glass pane was anticipated around a connection fitting due to local stress peaks (figure 4.5).

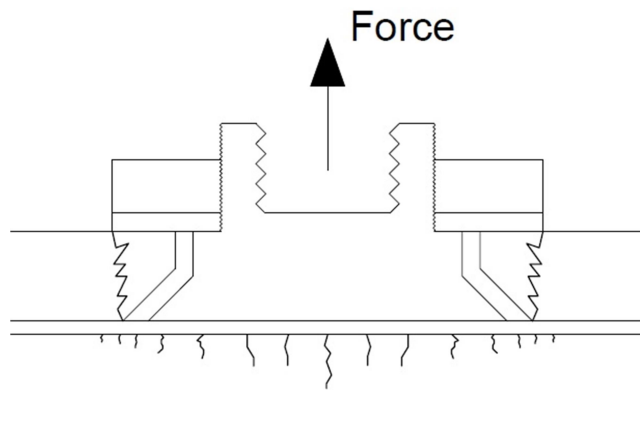


Figure 4.5 Glass failure

#### Foil – Fitting delamination

An adhesion failure was anticipated on the interface of a stainless steel connection fitting and Sentryglass foil due to reaching of a tear strength limit (figure 4.6).

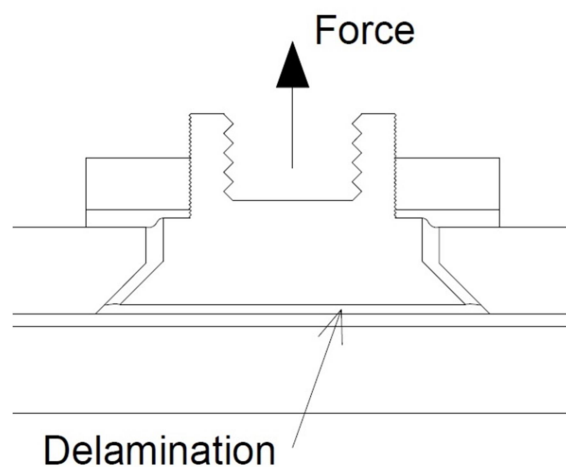


Figure 4.6 Delamination

### Interlayer foil failure

The last anticipated type of failure was a damage of an interlayer foil due to the normal stresses action (figure 4.7).

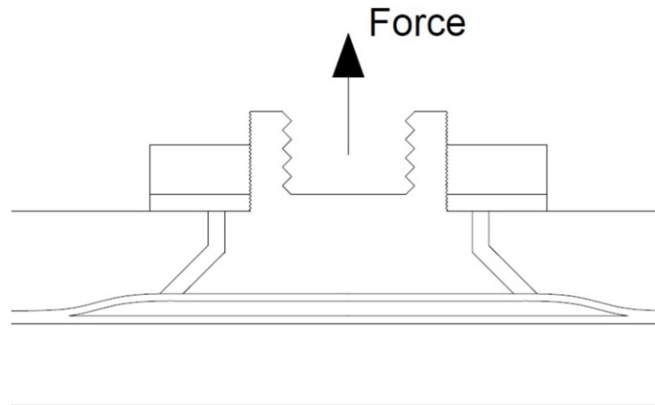


Figure 4.7 Interlayer foil failure

### 4.2. Tested specimens

The company OGB provided us with three sets of specimens. Each set is laminated with different type of foil and consists of three samples. This work focuses on the testing of the first set, laminated with ionoplastic foil (Sentryglass). The tested samples are marked F1-01, F1-02 and F1-03 (F1 = foil 1, 01 – 03 = number of specimen). The F1-01 sample can be seen in figure 4.8.

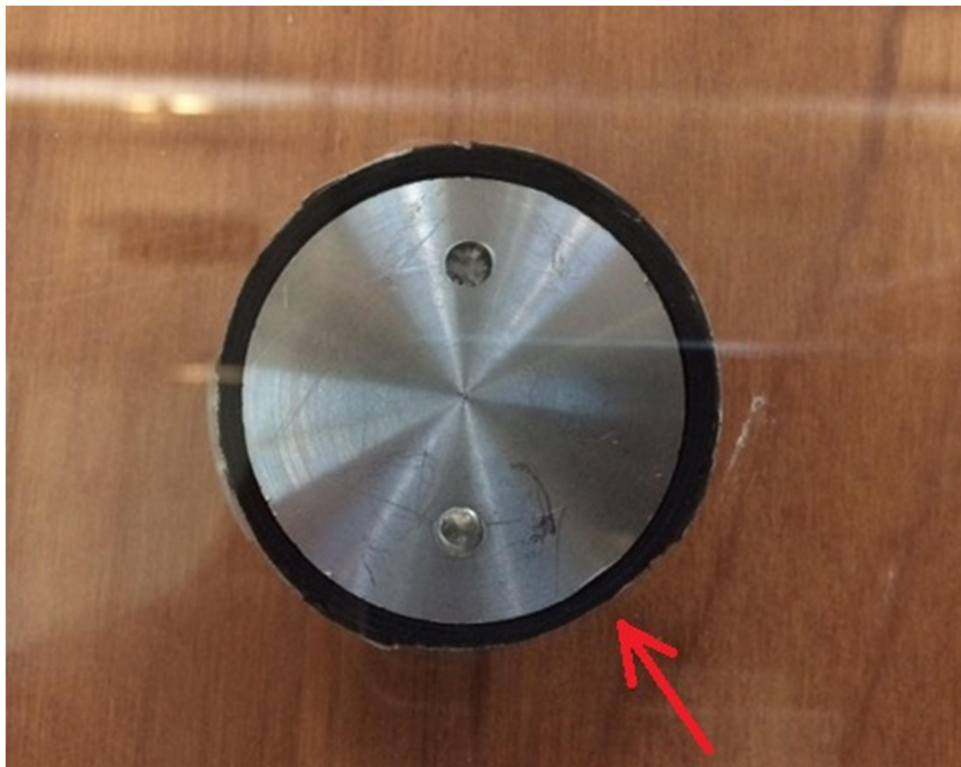


Figure 4.8 F1-01 sample

The samples from the set should be identical however each of them contains some flaws which should be pointed out.

#### 4.2.1. F1-01

The sample F1-01 does not have HDPE liner with uniform thickness around the connection fitting (figure 4.9). The connection fitting is also not ideally laminated as there can be bubbles seen around it (figure 4.10).



*Figure 4.9 The non-uniform thickness of a liner*

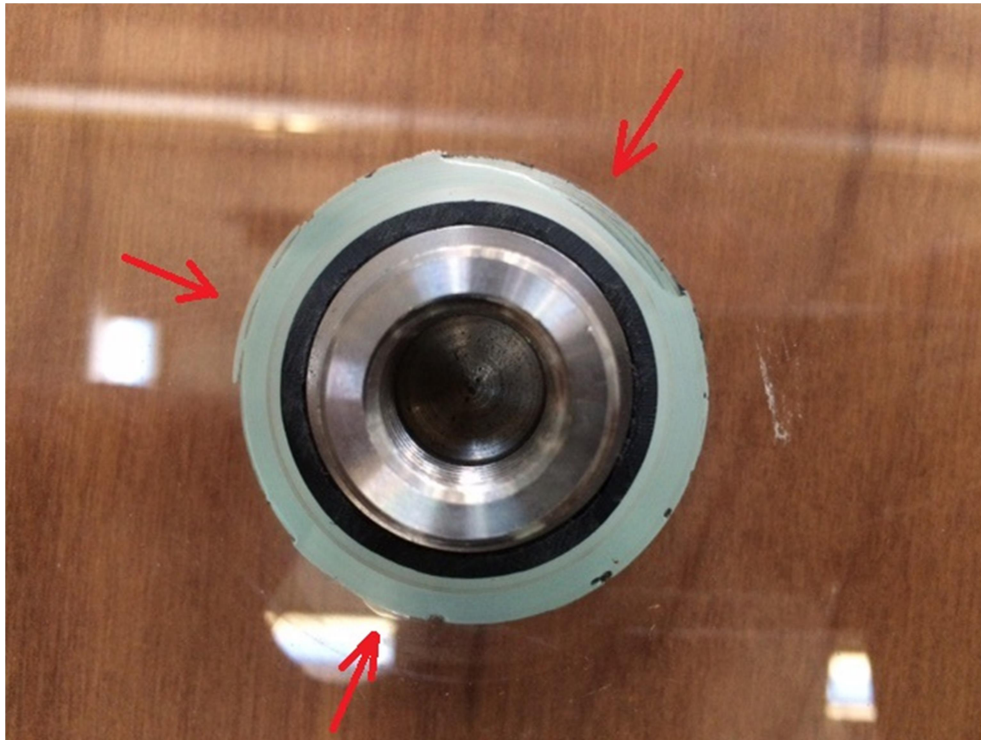


Figure 4.10 Bubbles around the connection fitting (F1-01)

#### 4.2.2. F1-02

The second sample from the first set has also the connection fitting not ideally laminated in. That can be seen on the connection's perimeter where a large group of bubbles and one single bubble occurs (figure 4.11).

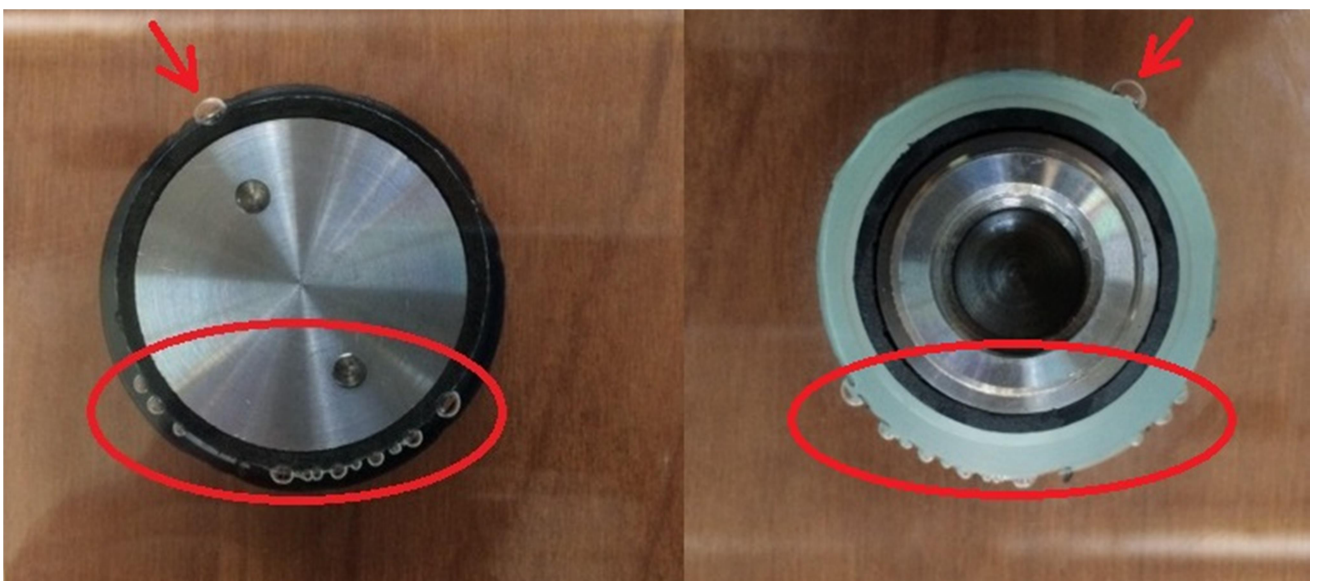


Figure 4.11 Bubbles around the connection fitting (F1-02)

#### 4.2.3. F1-03

The last sample from the first set has a non-uniform thickness of HDPE liner. There is also a small group of bubbles on the perimeter of the connection fitting. These flaws can be seen in figure 4.12. Apart from these flaws there is also a hairline scratch on the surface of the heat-strengthened glass pane (figure 4.13).

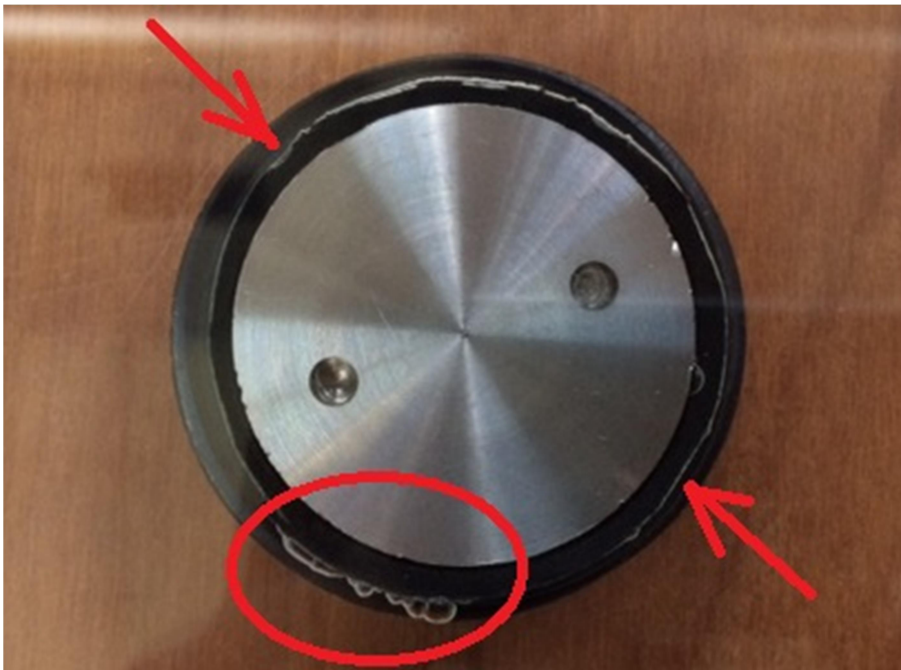


Figure 4.12 The non-uniform thickness of the liner and group of bubbles (F1-03)



Figure 4.13 Surface scratch (F1-03)

### 4.3. Testing equipment

In order to obtain the necessary data needed for the numerical model, the magnitude of load and deflection of the glass pane was measured during experiments. Also the type of the failure was observed. There is a brief description of equipment used in the following text.

#### 4.3.1. MTS QTest 100

The floor model testing frame with TestWorks 4 software was used to apply the loading to the glass pane. This model of test frame is equipped with the load cell and has loading capacity up to 100 kN.



Figure 4.14 MTS QTest 100

#### 4.3.2. EIR Laser Extensometer

The laser extensometer was used to measure the distance between the reference point and the M16 bolt connecting the load frame with the blind connection. Aluminum reflective tape was used as a target material for the laser.



Figure 4.15 The laser extensometer (left) and magnets with reflective tape (right)

#### 4.3.3. Steel Load Frame

As mentioned before the special load frame was used to apply the load to the tested specimens. It was designed to withstand the loading up to 50 kN.

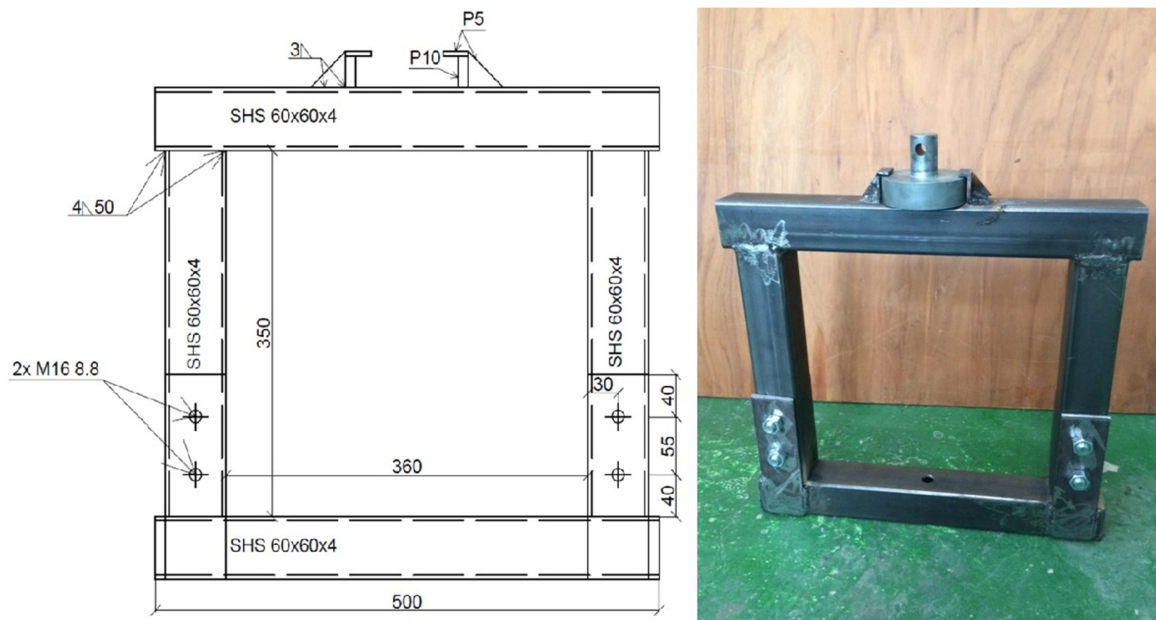


Figure 4.16 The sketch of the load frame (left) and the manufactured load frame (right)

#### 4.3.4. Steel Bed

A steel bed with maximum load capacity of 50 kN was used to support the cylindrical supports for the glass pane.



Figure 4.17 A steel bed with cylindrical supports and plastic washers

#### 4.4. Testing procedure

The main aim of the experiments was to test the samples under short-term tensional loading. Short-term loading was chosen deliberately to restrict the visco-elastic behavior of the interlayer foil as much as possible. Because of the same reasons the experiments were concluded in the temperature-stable environment with the temperature of 20°C. The testing included numerous loading and unloading cycles with 500 N or 1000 N load increments.

#### 4.5. Test results

For every experiment, deflection, load and type of failure was carefully noted. Apart from that also the time was recorded for the second and the third test for every loading or unloading step.

#### 4.5.1. F1-01

We had to be very careful during the first test because no one knew what to expect. There were eight full loading and unloading cycles before the first failure occurred in the ninth loading cycle. The course of stiffness of the glass pane with the connection was more or less linear as expected during the cycles with little portions of plastic deformations. Those are probably caused by use of plastic washers on the cylindrical supports of the pane and by the deformation of plastic liners around the stainless steel fitting.

Delamination of stainless steel fitting from the interlayer foil suddenly occurred at approximately ████ N. The fitting separated from the foil and started pressing against HDPE liners which lead to big increase of deformation. The deformation is clearly visible in figure 4.18 on the left – the HDPE liner is clearly not in contact with the glass pane above it. On the right side of the figure can be also seen that the delamination of the fitting is not recognisable from the outer side of the glass pane.

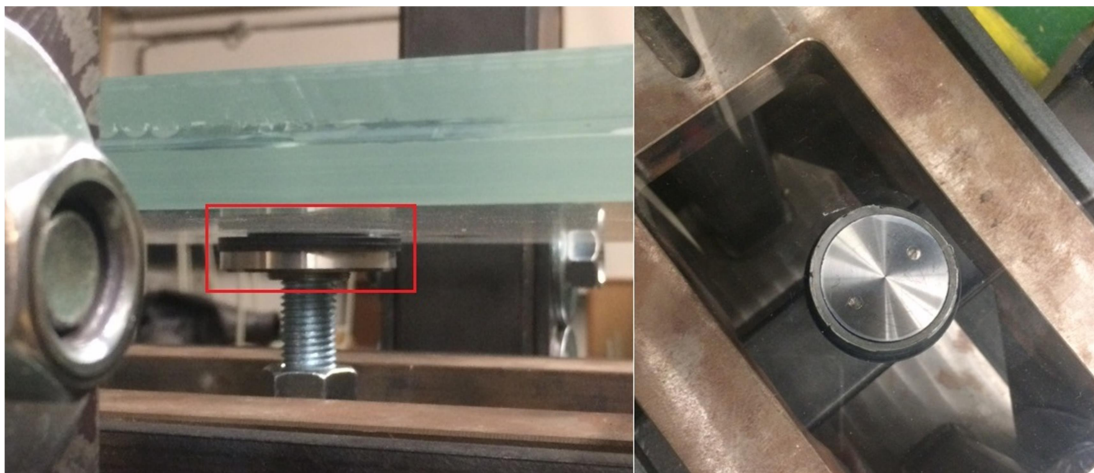


*Figure 4.18 Delamination of connection fitting (F1-01)*

After the delamination of the fitting the stiffness of the glass pane with the connection dropped but it was able to withstand additional loading. We were able to perform two full loading and unloading cycles so we could determine the stiffness after the fitting delamination.

After raising the load to approximately [REDACTED] N there was another sudden increment of deflection probably due to plastic deformation of the HDPE liners. The force dropped to [REDACTED] N but anything visible occurred on the sample.

The loading was slowly increasing up to the total failure of the connection which occurred at approximately [REDACTED] N. Shortly before the failure the delamination process started also at the glass – foil interface. It started very rapidly causing the perishing of the composite behavior of the laminated glass leading to the brittle failure of both glass panes (figure 4.19).



*Figure 4.19 Spreading delamination and brittle failure (F1-01)*

There was also partially ripped out the stainless steel connection fitting after the failure. This can be seen on figure 4.20.

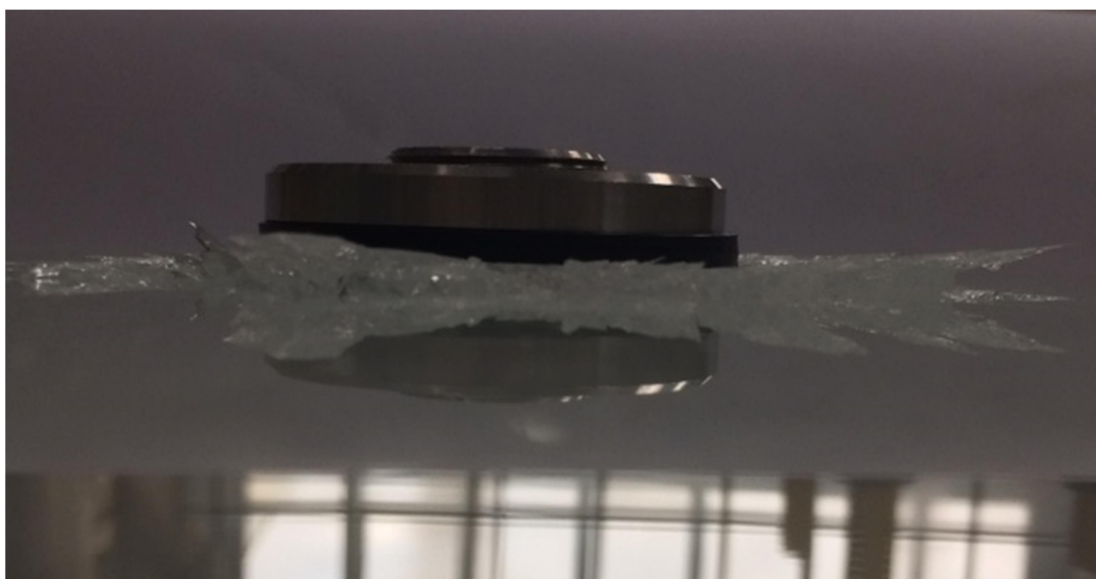
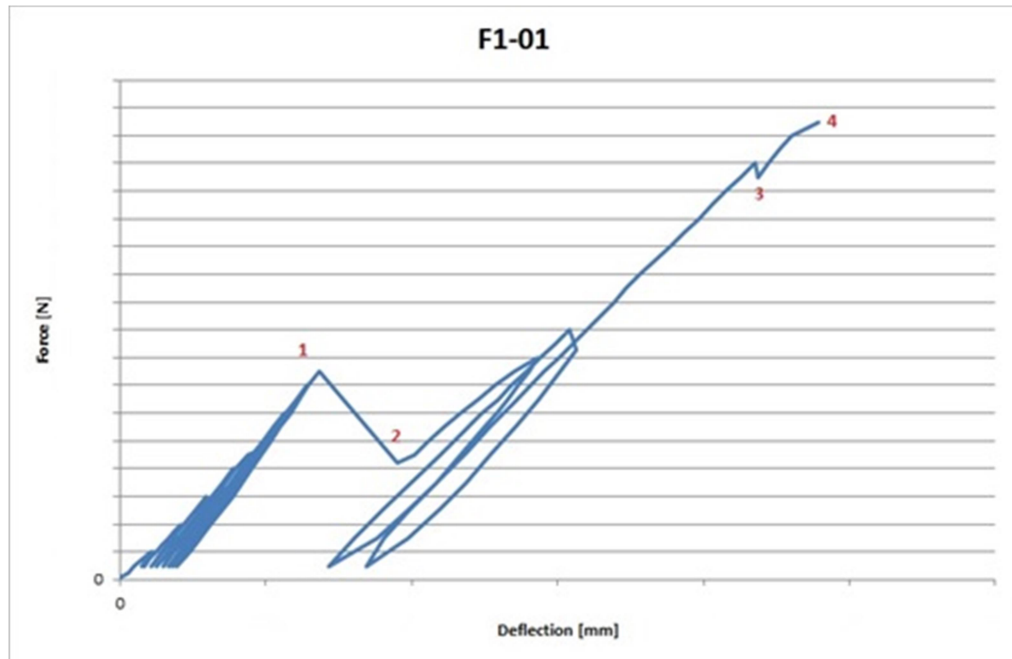


*Figure 4.20 Ripped out connection fitting (F1-01)*

The whole testing process can be seen on the following graph with description of the important points:

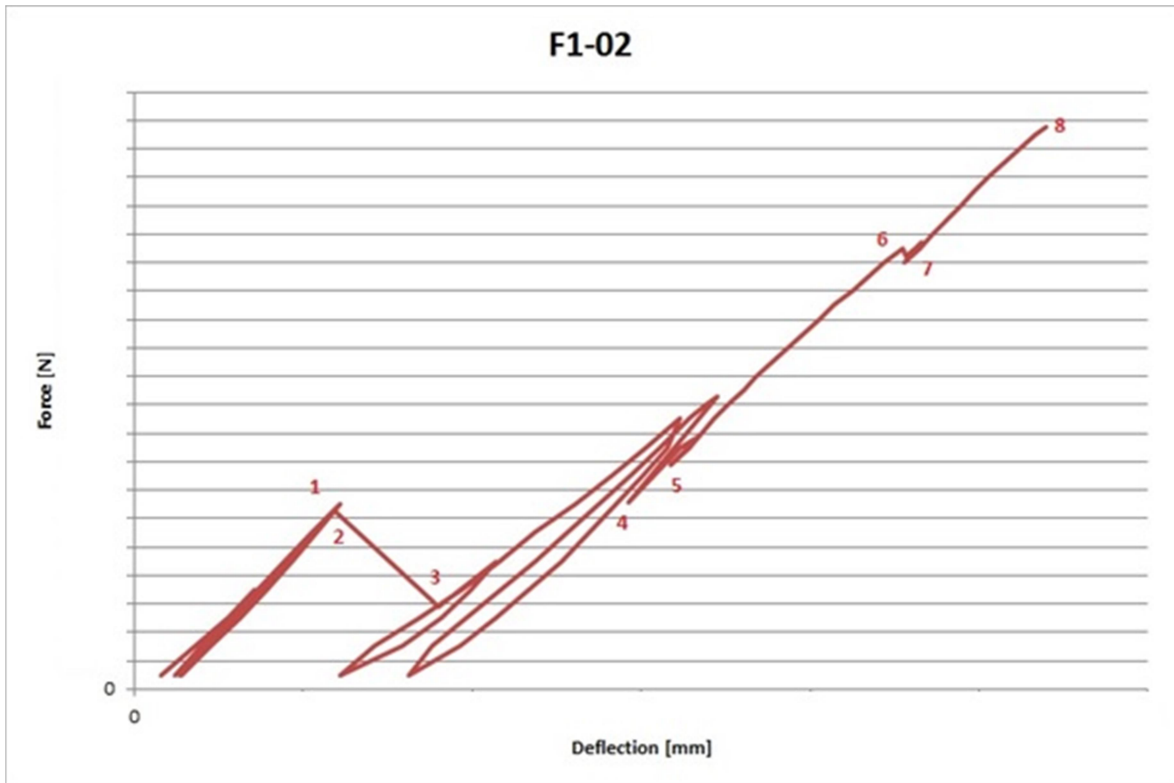


Graph 1 Force - deflection diagram (F1-01)

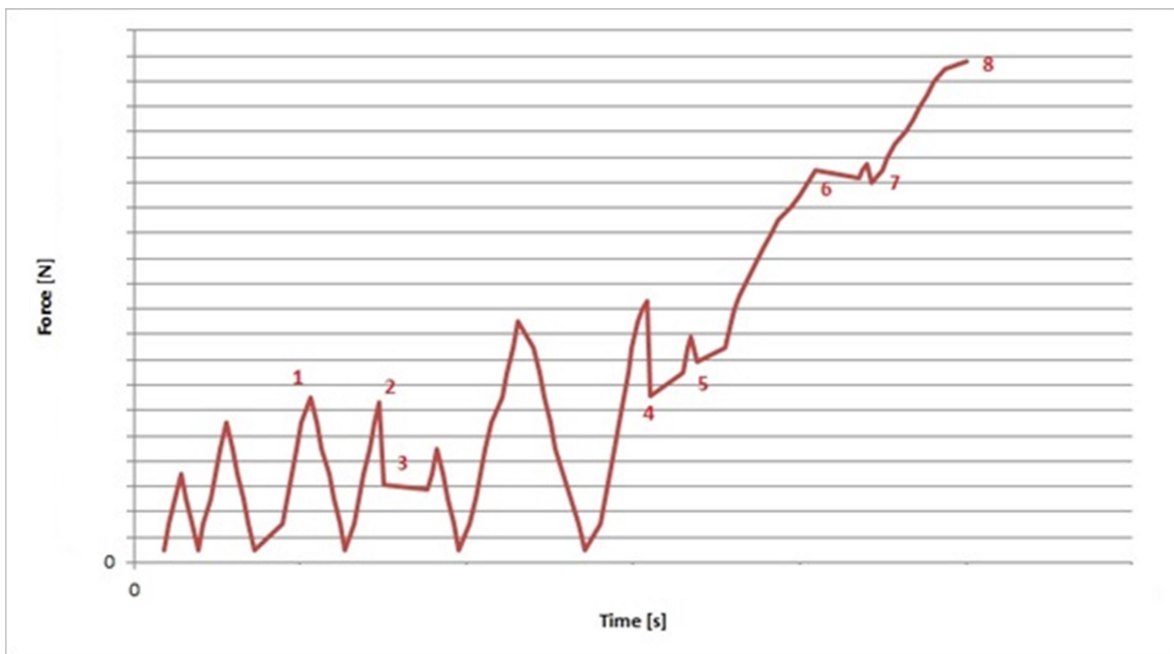
1. Delamination of stainless steel fitting from the interlayer accompanied by the decrease of original stiffness
2. Sudden increment of deformation
3. Deformation of HDPE liners
4. Brittle failure of glass panes

#### 4.5.2. F1-02

The testing of the second sample was conducted in the same manner as the first one however few differences appeared. Those will be shown and described in the following text.



Graph 2 Force - deflection diagram (F1-02)



Graph 3 Force - time diagram (F1-02)

1. Loading reaches to the prescribed value of [REDACTED] N and the unloading cycle starts
2. Loading cycle which was prescribed to increase the load up to [REDACTED] N is suddenly interrupted by fitting-foil delamination at approximately [REDACTED] N (figure 4.21)

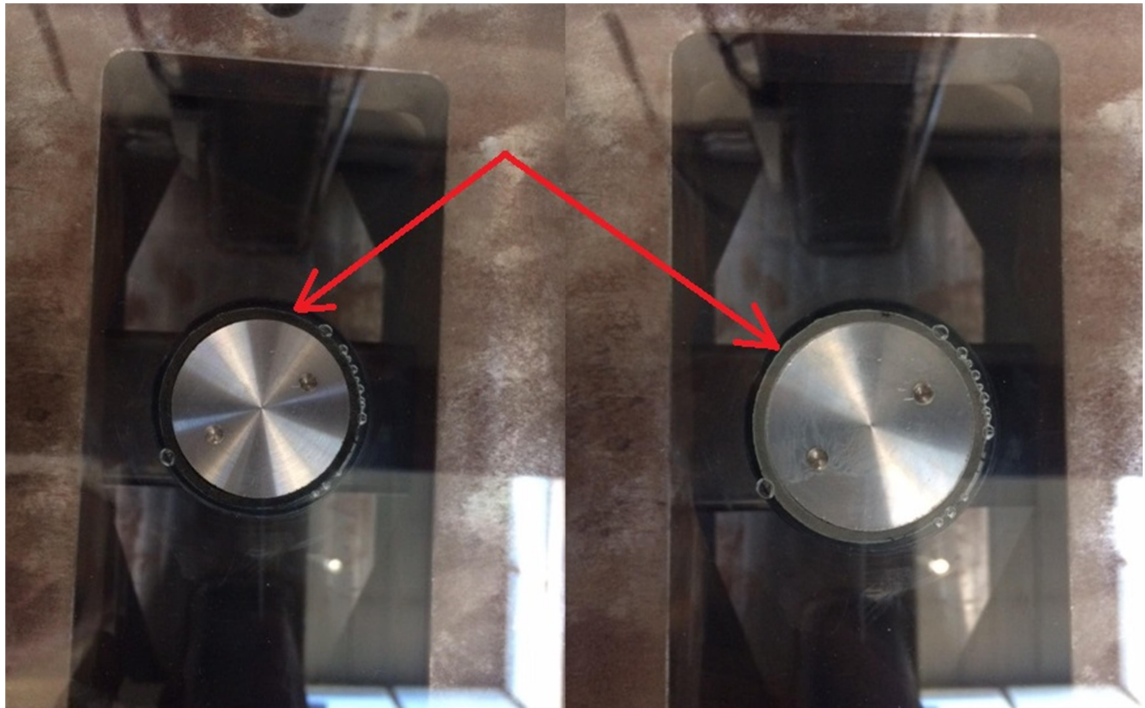


Figure 4.21 Foil-fitting delamination, note the change of color of the liner due to large air bubble inside (F1-02)

3. The delamination is quickly followed by increment of deflection
4. The loading cycle was interrupted by deformation of HDPE liners around the fitting
5. Same as the no. 4
6. Same as the no. 4
7. Same as the no. 4
8. Brittle failure of heat-strengthened glass pane (at approximately [REDACTED] N), the float glass pane remains intact

The mechanism of brittle failure remained the same as before – delamination started also on the glass-foil interface and was followed by losing of the composite behavior of the laminated pane. Unlike at the first sample it was clear here that the glass-foil delamination originated at the group of bubbles around the fitting (figure 4.22).



*Figure 4.22 Origin and the propagation of glass-foil delamination*

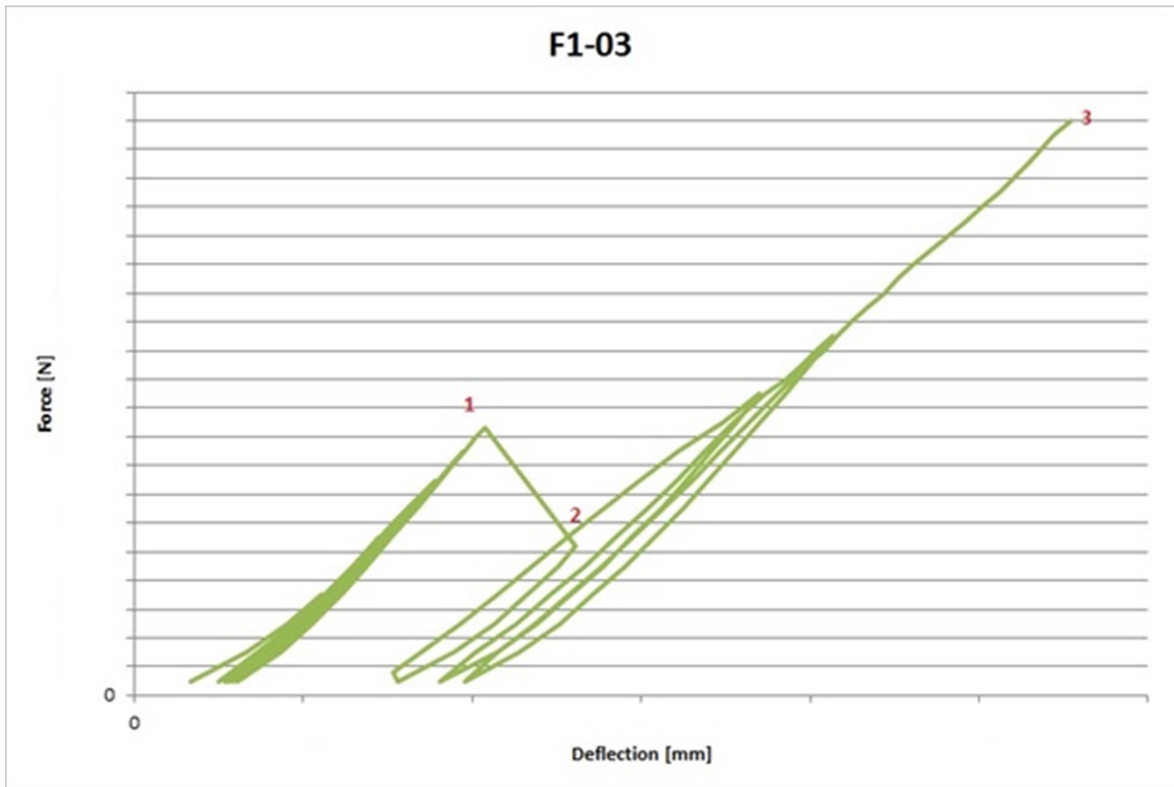
It should be also noted that only the heat-strengthened glass pane was destroyed and the connection fitting was ripped out completely (figure 4.23).



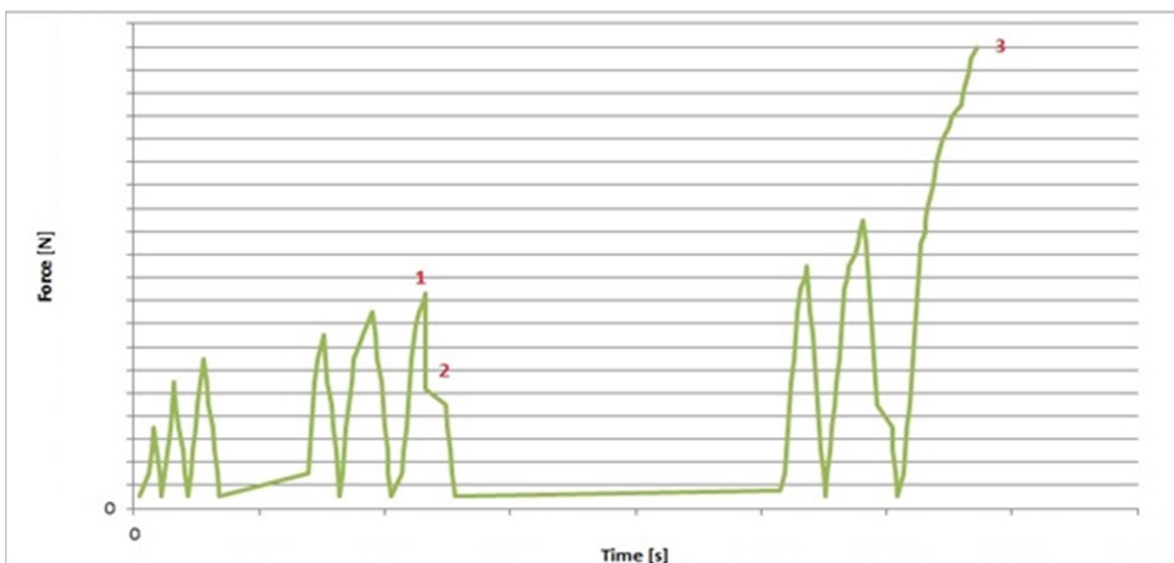
*Figure 4.23 Destroyed heat-strengthened glass pane with the connection fitting imprint, float glass pane is intact (F1-02)*

### 4.5.3. F1-03

The last experiment developed as the first one but as before with some minor differences. Here are the results of the last test.



Graph 4 Force - deflection diagram (F1-03)



Graph 5 Force - time diagram (F1-03)

1. Delamination of the connection fitting from the foil (at [REDACTED] N), this time it is clearly visible as an air bubble forms in between the fitting and the foil (figure 4.24)



Figure 4.24 Foil-fitting delamination (F1-03)

2. Increment of deflection and drop of the force to [REDACTED] N
3. After two full loading and unloading cycles, the laminated glass pane fails at approximately [REDACTED] N. The delamination on the glass – foil interface occurred shortly before the brittle failure as before (figure 4.25).



Figure 4.25 Glass-foil delamination (F1-03)

Same as before at the second test the brittle failure occurred only in heat-strengthened glass pane while the float glass pane remained intact. Also the connection fitting was completely ripped out from the damaged glass pane (figure 4.26).

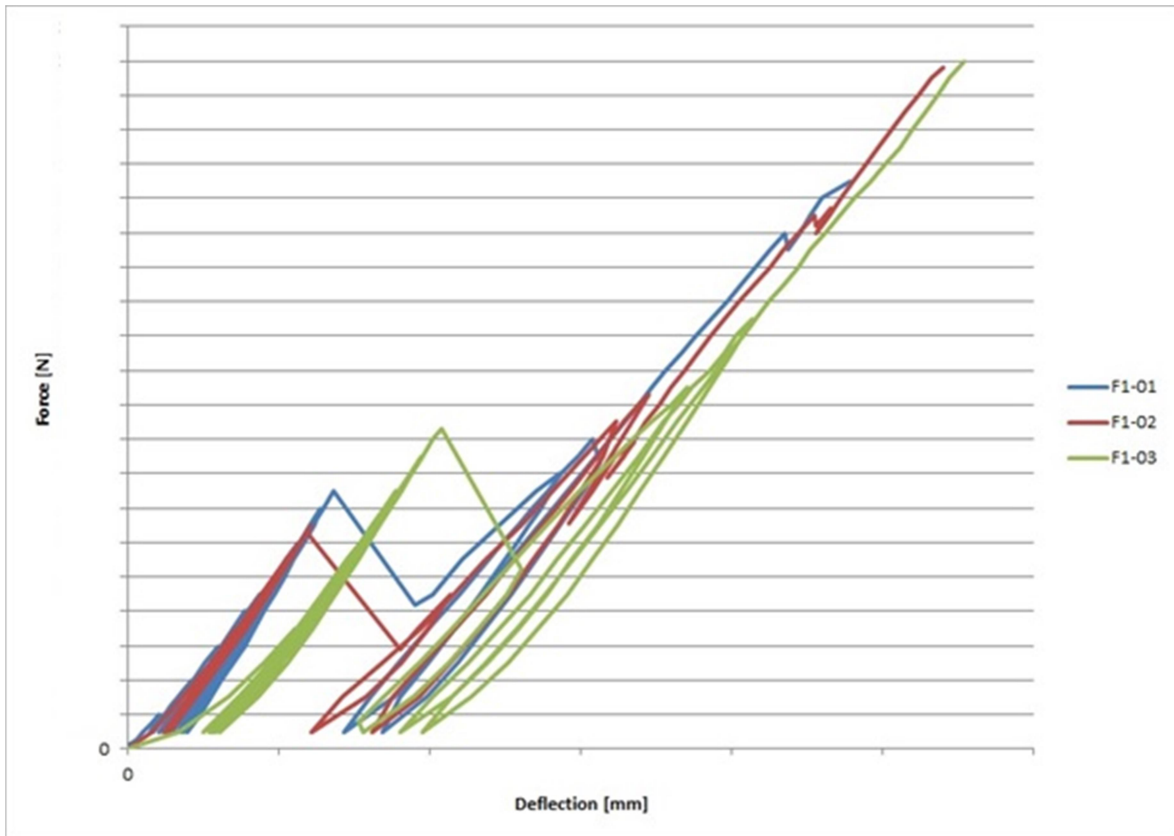


*Figure 4.26 Destroyed heat-strengthened glass pane with the connection fitting imprint, float glass pane is intact (F1-03)*

Unlike in the two earlier tests any additional deformation of HDPE liners did not occur here after the connection fitting delamination.

#### **4.5.4. Evaluation of experiments**

Comparison of experiments as well as calculation of different values of stiffnesses was performed. The stiffness resemblance of each sample as well their load-bearing capacity can be seen in graph 6.



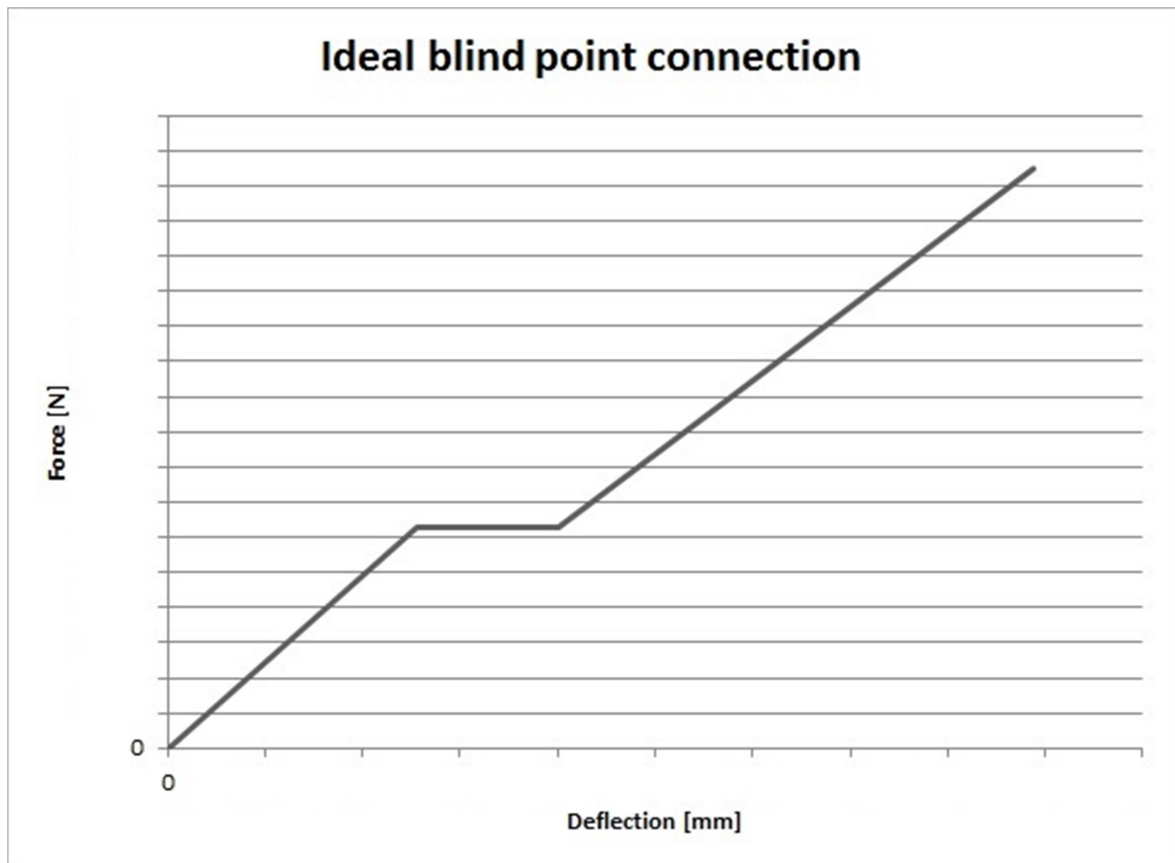
Graph 6 Force-deflection diagram of all samples

There is also a table where all the important data can be easily compared. The stiffnesses in the table are already average values taken from three or more loading or unloading cycles.

Sample	Force [N]	Deflection [mm]	Stiffness [N/mm]
F1-01	...	...	...
F1-02	...	...	...
F1-03	...	...	...

Table 2 Values obtained from the experiment data

The values highlighted in green in the table 2 were used for construction of an ideal behavior blind point connection diagram which is shown below.



Graph 7 Force-deflection diagram of ideal blind point connection

#### 4.5.5. Conclusion

All three samples had the same failure mechanism. The first failure was always the delamination of the connection fitting from the foil, followed by the drop of the stiffness. The total failure was again initiated by a rapid glass-foil delamination shortly before the loss of composite behavior and brittle failure.

The point in which the connection fitting-foil delamination occurs is still unpredictable and research should be conducted on the larger scale to establish a method of identifying that point. It should be noted that according to the producer of samples the stainless steel fittings were not treated in any way. It is my recommendation to treat at least the contact surface of the connection fitting (in contact with interlayer foil) by degreasing and by making sure that the contact area of each fitting is the same (no scratches, bumps etc.). These measures should provide us with more exact values of the force needed for delamination of the connection fitting.

In practical use of this type of connection I would primarily recommend to inspect these connections on regular basis to avoid the brittle failure. It is obvious from the graphs that this type of connection has a tremendous residual capacity nevertheless it should be replaced after the connection fitting delamination. The signs of failure would be:

- Change of color of liners due to large air bubbles (figure 4.21)
- Large bubbles on the contact surface (figure 4.24)
- Tightening nut (and liner) not in contact with the inner glass pane (figure 4.18)

## 5. Numerical analysis

The last part of this thesis is to create a finite element model of the tested connection, determine its important characteristics and use them to prepare a parametric study of such connection with chosen parameter.

There is a wide range of software suitable for this task nowadays with free student licenses available. The software which was used for the modeling is ANSYS Workbench 16.2 (student version), namely its static structural analysis system.

### 5.1. Numerical model

A three-dimensional numerical model was prepared to simulate the behavior of tested specimens. The main goal is to reach such behavior which is shown in graph 7 to the point of the delamination of the stainless steel connection fitting.

#### 5.1.1. General conditions

Due to the symmetry of tested specimens only quarter of the sample was modeled. This contributes to a downsizing of a problem leading to a better computational speed. It also means that three boundary conditions had to be used instead of two. These are depicted

in figure 5.1. Please note that 2D representation was used for clarity of the problem. The supports are always applied to surfaces (whole sides of specimen) and arrows in the vicinity of supports show the directions of allowed movement.

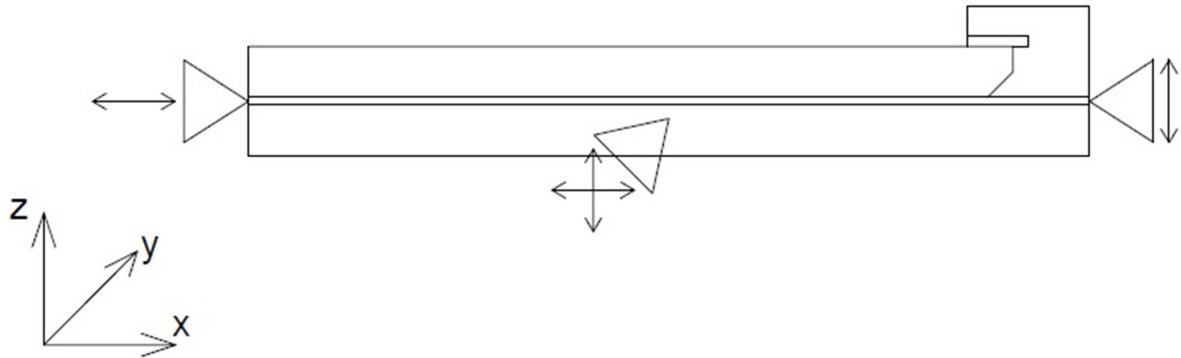


Figure 5.1 FE model boundary conditions

Cohesive zone modeling had to be used to include delamination of the connection fitting into the model. Debonding property of bonded contact surface-to-surface elements was used here, namely separation-distance based debonding (figure 5.2).

Properties of Outline Row 3: CZM				
	A	B	C	D E
1	Property	Value	Unit	
2	Separation-Distance based Debonding			<input type="checkbox"/>
3	Debonding Interface Mode	Mode I		
4	Tangential Slip Under Normal Compression	No		
5	Maximum Normal Contact Stress		MPa	<input type="checkbox"/>
6	Contact Gap at the Completion of Debonding	0,3	mm	<input type="checkbox"/>
7	Maximum Equivalent Tangential Contact Stress		Pa	<input type="checkbox"/>
8	Tangential Slip at the Completion of Debonding		m	<input type="checkbox"/>
9	Artificial Damping Coefficient	1E-08	s	<input type="checkbox"/>

Figure 5.2 Separation-distance based debonding

This method requires use of virtual material (cohesive zone material) with certain properties. Input parameters needed for this material are:

- Debonding Interface Mode = Mode I (separation in normal direction)
- Maximal Normal Contact Stress = numerical value [MPa]

Value of  $\blacksquare$  MPa as the input corresponds to delamination of the connection fitting under the load of  $\sim \blacksquare$  kN. The delamination in the experiments occurred suddenly but in the FE model is taking place gradually. That is why the first occurrence of this value at the contact surface is taken as a sign of delamination failure. This can be observed in figure 5.3.

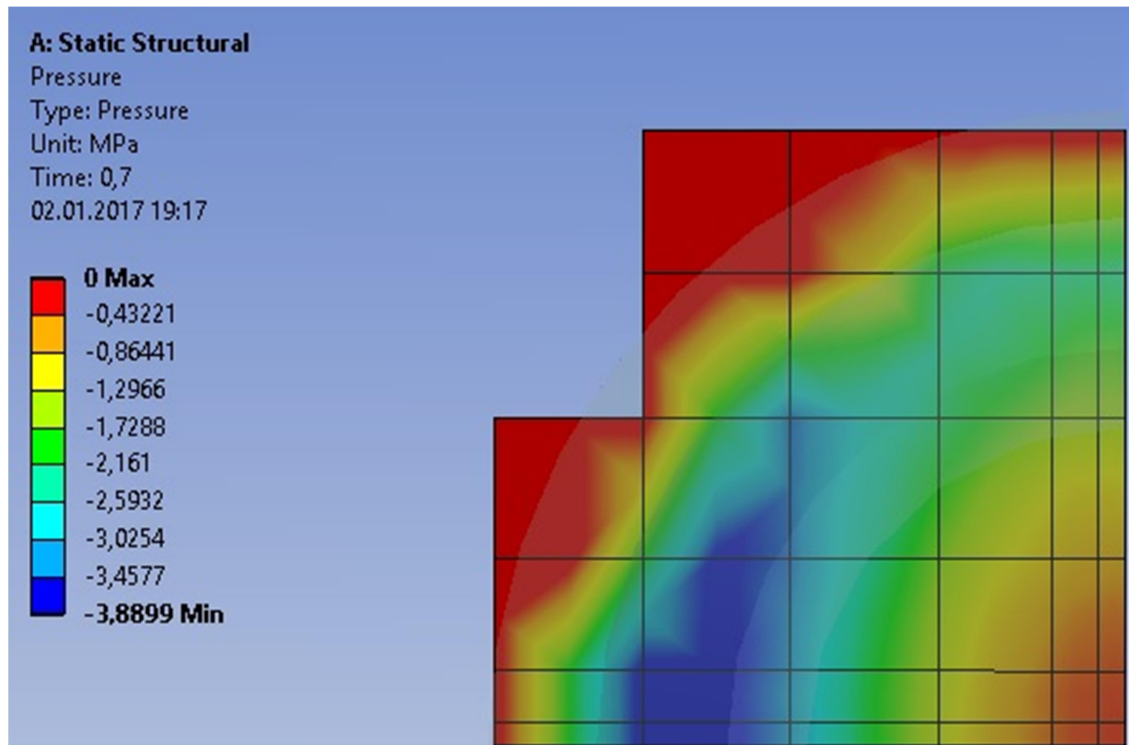


Figure 5.3 Delamination – contact stress

- Contact Gap at the Completion of Debonding = numerical value [mm]
- Artificial Damping Coefficient = numerical value [s]

Debonding is usually accompanied by convergence difficulties in the solution. Artificial damping coefficient is set up to help stabilize the solution. Its value must be smaller than minimum time step size [15].

The delamination itself can be seen in figure 5.4. The delamination corresponding to the figure 5.3 is on the left. Then it gradually spreads as mentioned before (right).

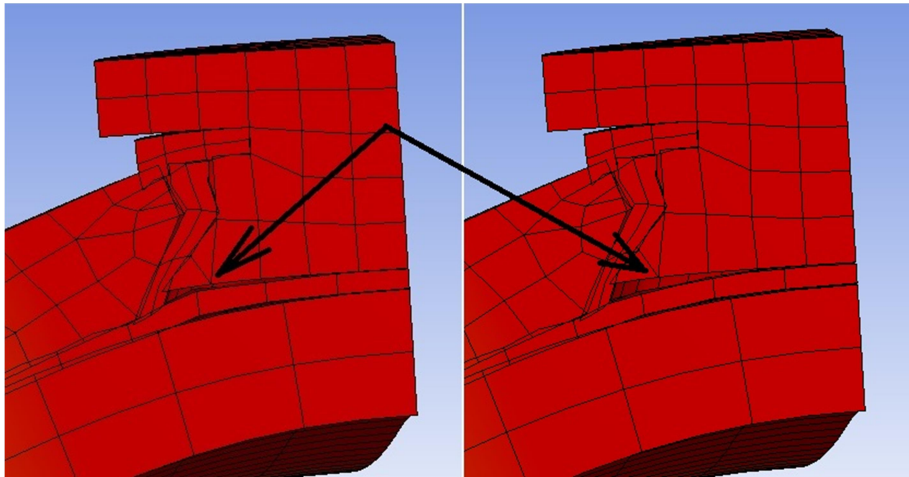


Figure 5.4 FEA delamination

### 5.1.2. Model geometry

Only quarter of the problem was modeled due to its symmetry as mentioned before. The model consists of six bodies. There are two glass panes, stainless steel connection fitting, interlayer foil, and two pieces of HDPE liners. The part of glass panes outside the cylindrical support is not considered in the model – only 165 mm from the center to the cylindrical support was modeled. This means the size of the laminated glass pane model is 165 mm x 150 mm. This can be clearly seen in figure 5.9.

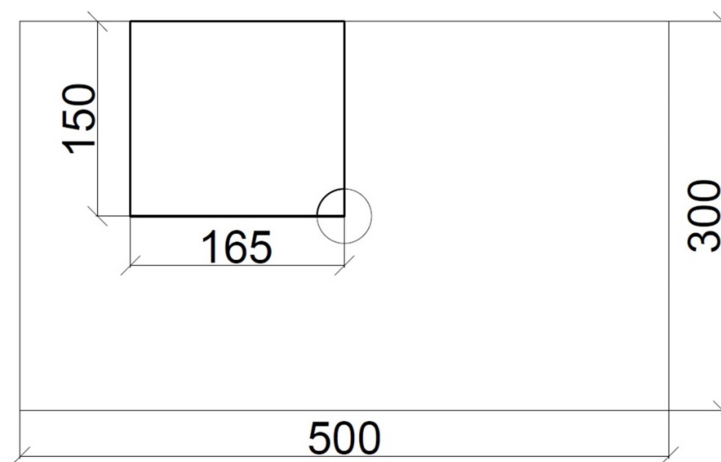


Figure 5.5 Scheme of the model (experiment - thin line, model - thick line)

The connection fitting was modeled without the inner thread as there is a bolt threaded in during its use (figure 5.11). The connection fitting hole in the heat-strengthened glass pane has a diameter which is 2 millimeters bigger than the connection fitting's one.

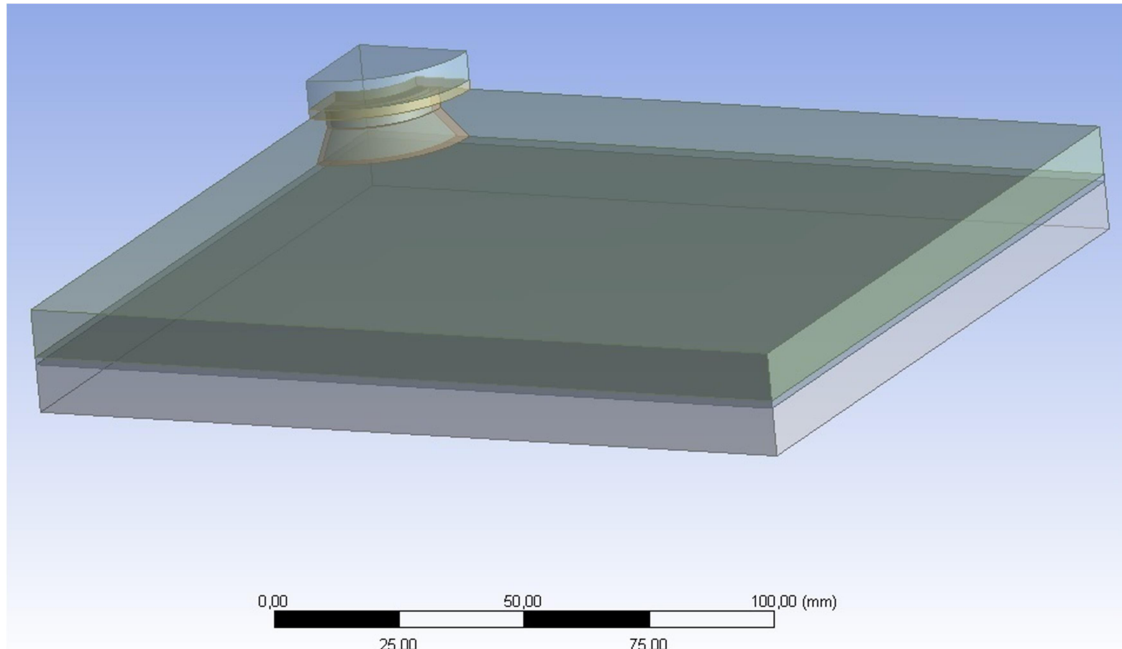


Figure 5.6 Geometry of the model

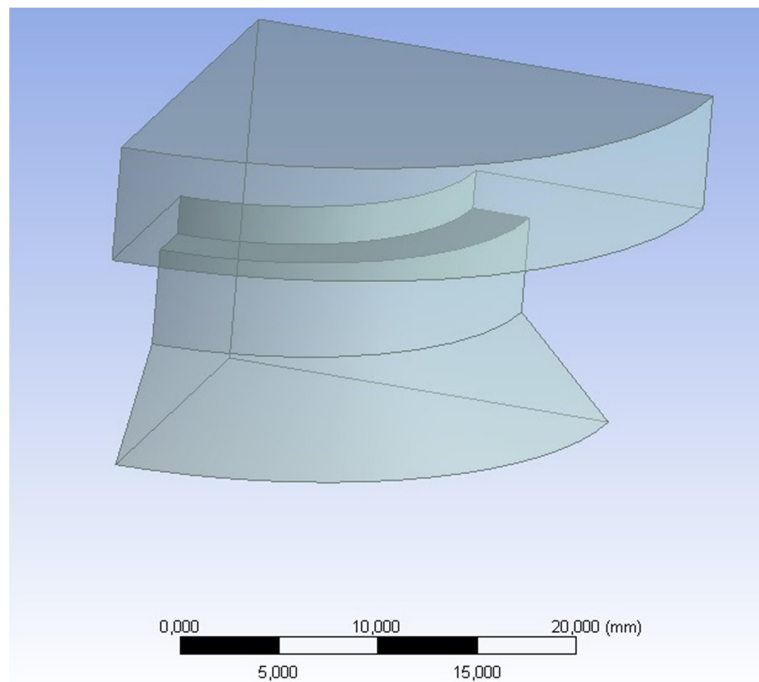


Figure 5.7 Model - detail of the connection fitting

### 5.1.3. The meshed model

Here is a list and a brief description of elements used in the numerical analysis:

#### SOLID185

Element SOLID185 was used to model glass panes and stainless steel connection fitting. It is a 3D element with eight nodes. Each node has three degrees of freedom – translation in x, y and z direction [15].

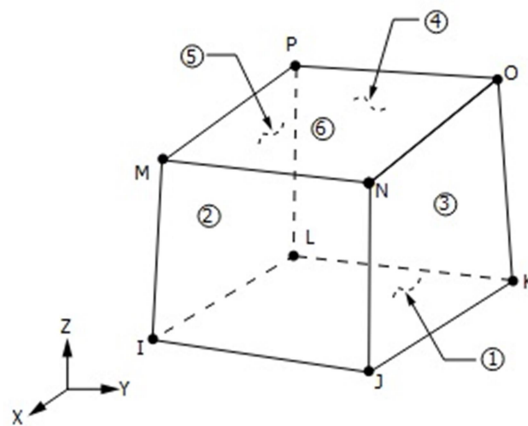


Figure 5.8 SOLID185 finite element [15]

#### SOLID186

SOLID186 is a higher order 3D element. It has twenty nodes with three degrees of freedom (translations in all three directions) [15]. These elements were used for modeling of 'soft' materials in the FE model (HDPE, interlayer foil).

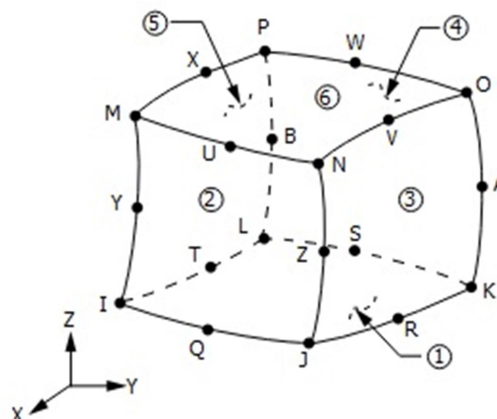


Figure 5.9 SOLID186 finite element [15]

### CONTA174

This is an element used to define a deformable surface which is in contact with its target surface [15].

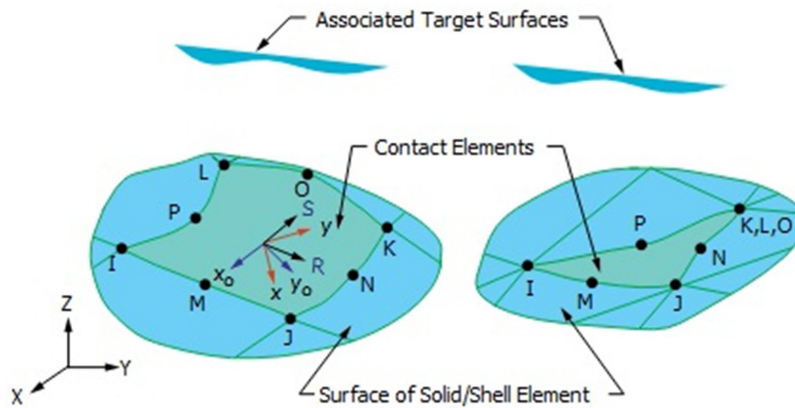


Figure 5.10 CONTA174 finite element [15]

### TARGE170

TARGE170 is an element which defines a 3D target surface associated with other contact elements [15]. TARGE170 is associated with CONTA174 in this case.

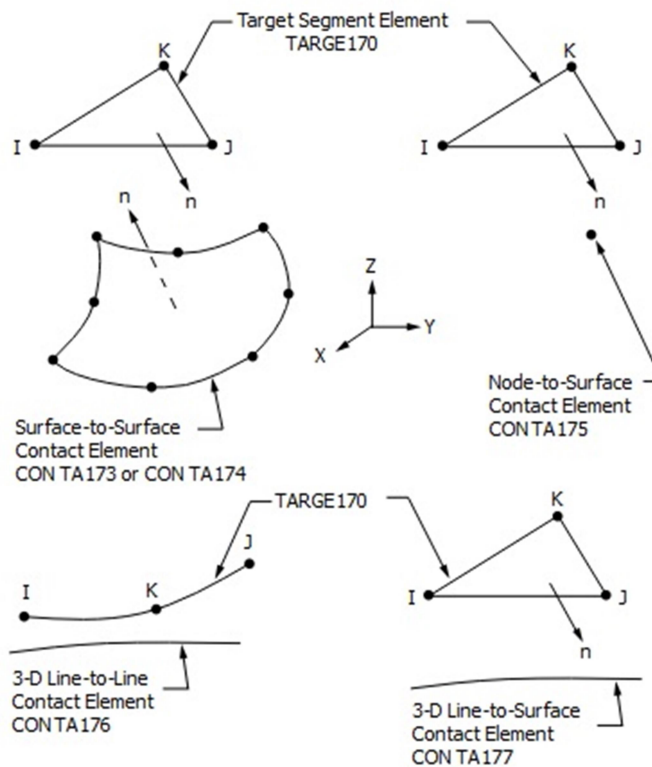


Figure 5.11 TARGE170 finite element [15]

The meshing of the model was performed with the elements described before. There is a size limitation of the problem due to use of a student version of ANSYS Workbench to 32000 nodes. The final mesh can be seen in figure 5.12. The mesh consists of 27749 nodes and 14188 elements.

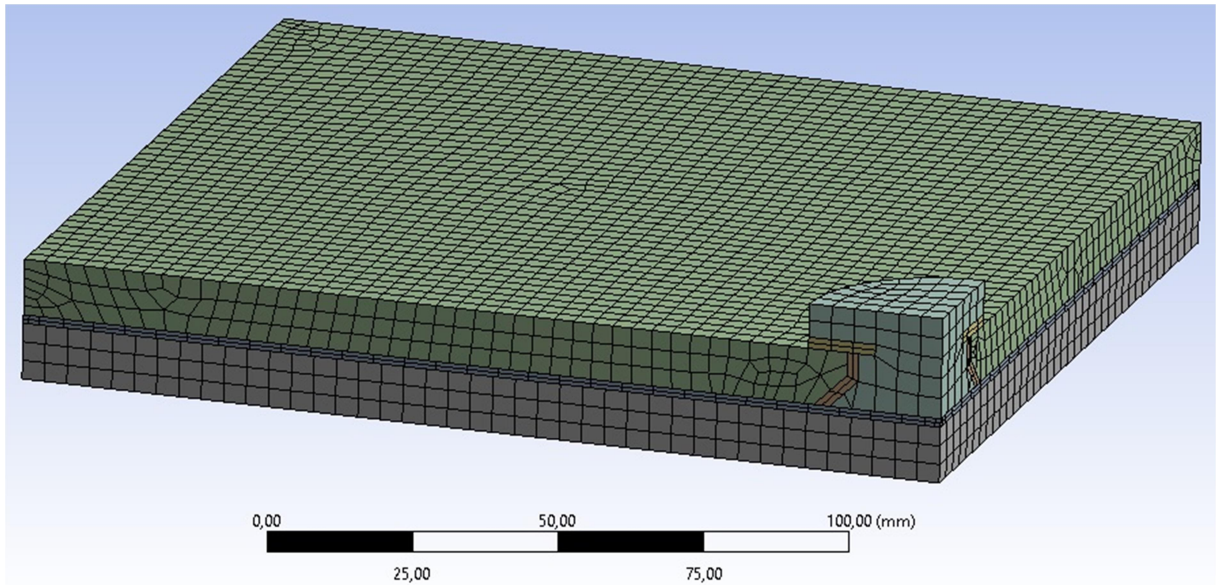


Figure 5.12 The meshed model

#### 5.1.4. Material properties

There will be a brief description of properties of all materials used in experiments and numerical analysis. Each property of each material has two values – one that was used in the numerical analysis and one that is typically used. The red color indicates the inequality between them.

Glass

	FEA	typical
$\rho$ [kg/m <sup>3</sup> ]	2500	2500
E [MPa]	75000	70000
$\nu$ [-]	0,23	0,23
G [MPa]	30048	26200
$f_{t, \text{float}}$ [MPa]	45	45
$f_{t, \text{heat-str.}}$ [MPa]	100	80 - 100

Table 3 Material properties of glass (FEA x typical)

It can be seen that higher modulus of elasticity thus shear modulus was used (because value of Poisson's ratio was kept the same) here in order to achieve the desired stiffness of the model. Typically 70000 MPa is used in static calculations of glass structures but according to [5] range of values of elastic modulus for glass is 70000 – 74000 MPa. The value used in the numerical analysis is then chosen reasonably.

#### High density polyethylene

	FEA	typical
$\rho$ [kg/m <sup>3</sup> ]	950	950
E [MPa]	1100	1100
$\nu$ [-]	0,42	0,42
G [MPa]	387	387

*Table 4 Material properties of HDPE (FEA x typical)*

Typical properties were used in the numerical analysis for high density polyethylene since nothing required their adjustment.

#### Stainless steel

	FEA	typical
$\rho$ [kg/m <sup>3</sup> ]	7750	7750
E [MPa]	193000	193000
$\nu$ [-]	0,31	0,31
G [MPa]	73664	73664

*Table 5 Material properties of stainless steel (FEA x typical)*

Typical properties were also used for the stainless steel material in the numerical analysis.

## SentryGlass

	FEA	typical
E [MPa]	1500	628
$\nu$ [-]	0,448	0,448
G [MPa]	518	217
$f_t$ [Mpa]	34,5	34,5

Table 6 Material properties of SentryGlass (FEA x typical)

Material representing the SentryGlass foil in the numerical analysis had to be modified in order to provide the measured value of stiffness of real samples. The typical values of properties in the table were obtained in the catalogue of the producing company [16]. These are values valid for  $T = 20^\circ\text{C}$  and  $t$  (load duration) = 1 s. When using these values the stiffness  $k$  of such model is 8,97 kN/mm although the stiffness of real samples is at least  $k = \blacksquare$  kN/mm (table 2). That means that by using of typical values of modulus of elasticity and shear modulus provided by the producer, we do not get the shear connection that was observed during the experiments. From that reason the modulus of elasticity  $E$  was raised to 1500 MPa and consequently the shear modulus  $G$  to 518 MPa as the Poisson's ratio was kept at its typical value.

### 5.1.5. Calculation procedure

When having the mesh done and materials characteristics set up there is few last conditions left to be done (figure 5.13):

- Connections

Nine connections between bodies had to be made. Bonded contacts were applied among glass panes and interlayer and between connection fitting and the interlayer. All the other connections were configured as No Separation contacts.

- Boundary conditions

These were already mentioned and explained in the chapter 5.1.1 (figure 5.1).

- Loading

Although the loading was recorded as a force in the experiment, the surface pressure was used in the numerical model instead. The reason for doing this is to avoid the nodal stress peak in the place of applied force. The surface on which is the loading applied can be seen in figure 5.13. The pressure is then recalculated back to force in the result chapter.

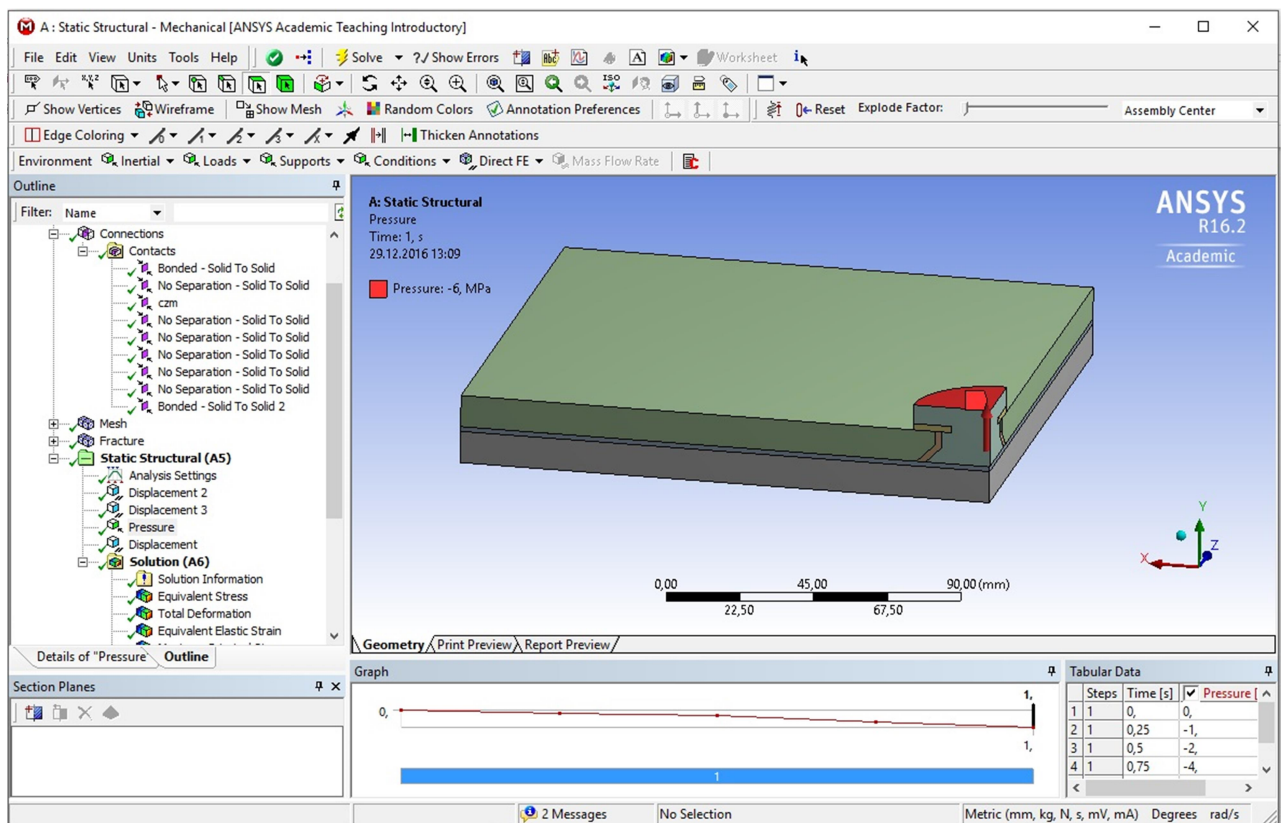


Figure 5.13 ANSYS static structural

## 5.2.Results

Static structural analysis was performed with the introduced numerical model. Deformation of the model corresponds to both expectations and experiments and can be observed in figure 5.14. Contact stress in between the connection fitting and SentryGlass interlayer suggests that the delamination failure will occur while load = ██████ kN and deflection = ██████ mm. The contact stress  $\sigma_{delam}$  was already identified to be ██████ MPa.

The detail in figure 5.15 shows the opening gap on the connection fitting – interlayer foil interface.

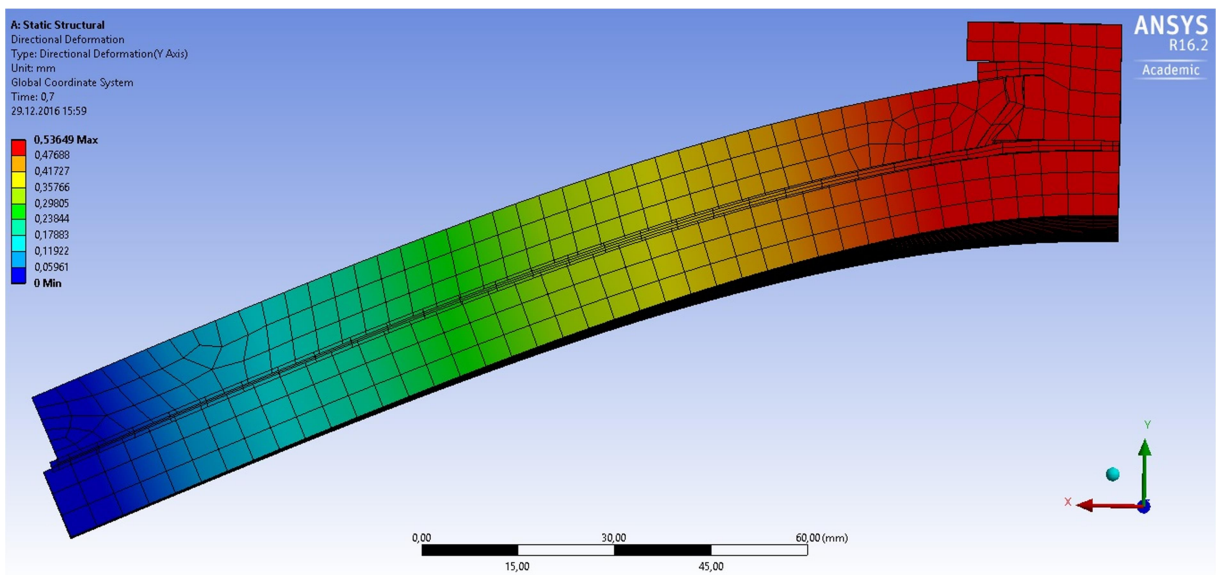


Figure 5.14 Deformation of the model

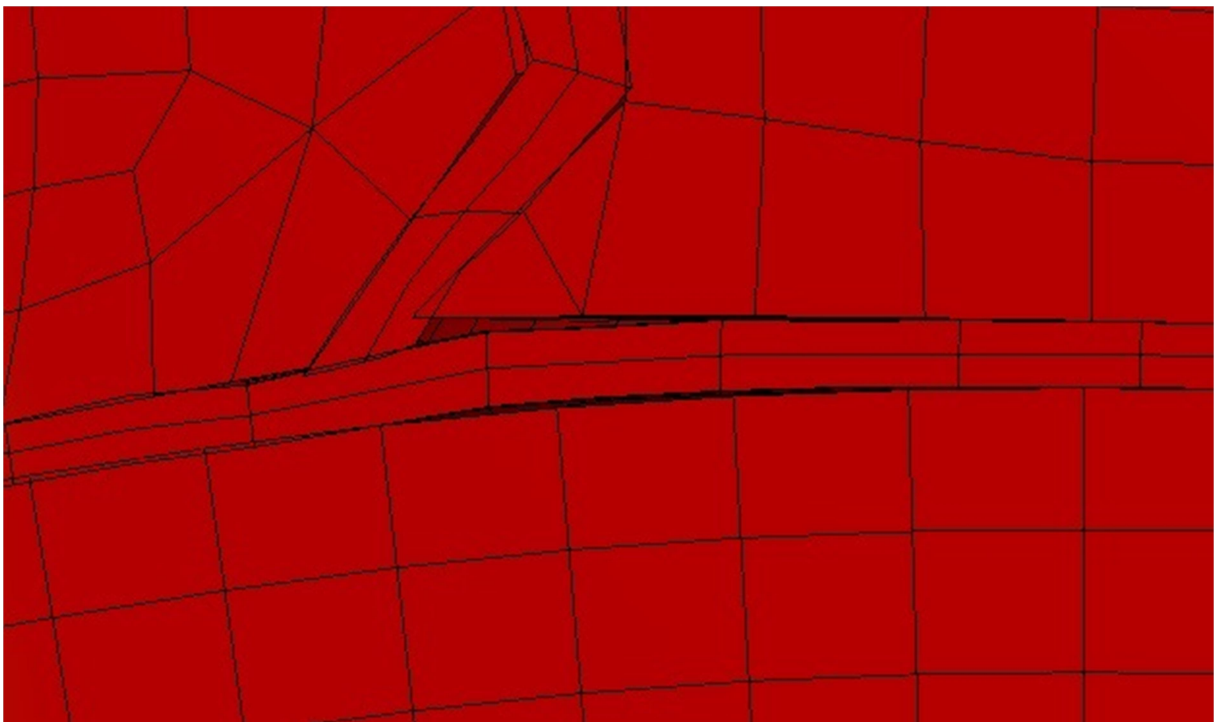
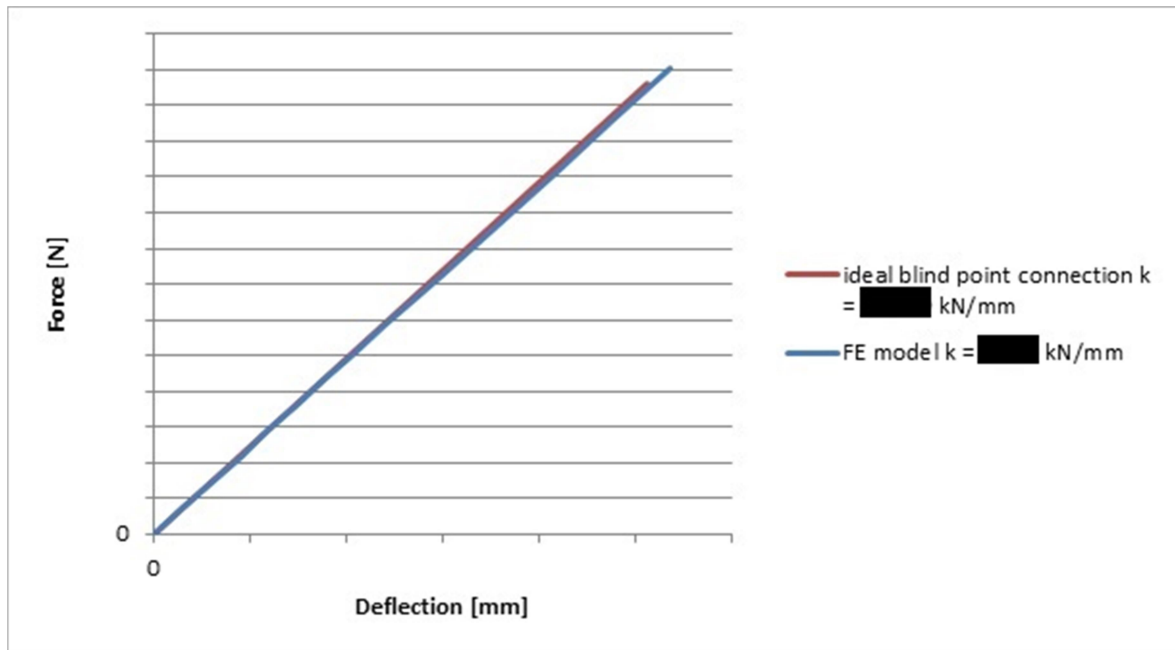


Figure 5.15 Gap opening on the connection fitting - interlayer foil interface

Stresses in glass panes or the interlayer foil do not indicate any possible failure due to overreaching tensional or compressive strength of those materials. The stiffness of the model  $k = \blacksquare$  kN/mm corresponds with the proposed ideal blind point connection where  $k = \blacksquare$  kN/mm (graph 7). The comparison between the result and the proposed ideal behavior of the connection can be seen in graph 8. The result clearly proves that material characteristics used in the numerical model correspond to reality.



Graph 8 Force-deflection graph of pre-delamination behavior

The important characteristics of the FE model are summarized and compared with the ideal blind point connection in the table below for the more detailed observation.

	FE model	Ideal blind point conn.
$F_{delam}$ [kN]		
$\sigma_{delam}$ [MPa]		
$\delta_{delam}$ [mm]		
$k$ [kN/mm]		

Table 7 FE model x ideal blind point connection

### 5.3. Parametric study

The existing numerical model was modified and used to create four new ones with different geometry in order to perform a simple parametric analysis.

#### 5.3.1. Description

The diameter of the contact area was the variable parameter of this study – ranging from 30 mm up to 70 mm. The height of the connection fitting remained the same as all the dimensions in the vertical direction. The dimensions in horizontal direction were scaled up or down accordingly in order to keep the same ratio between the diameter of the contact area and other dimensions (figure 5.16).

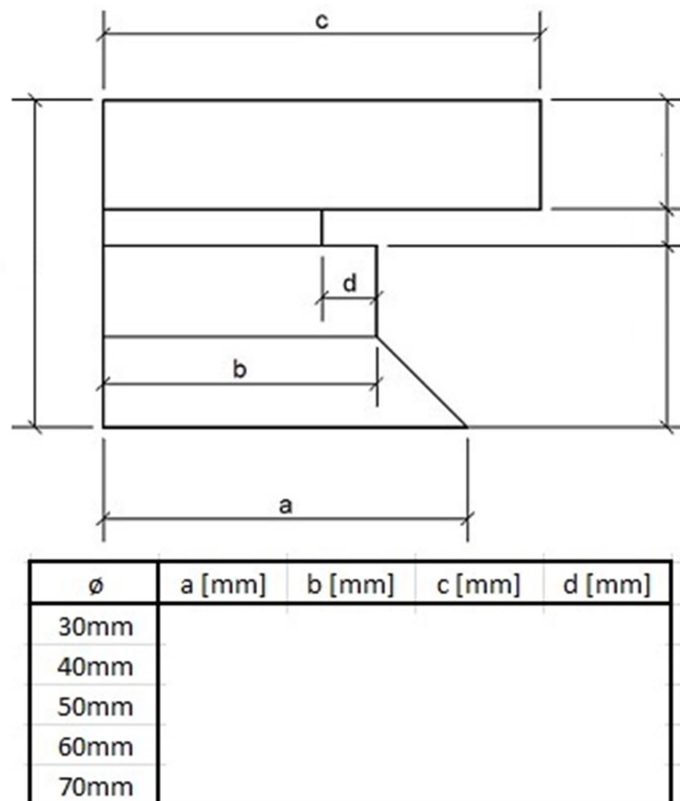
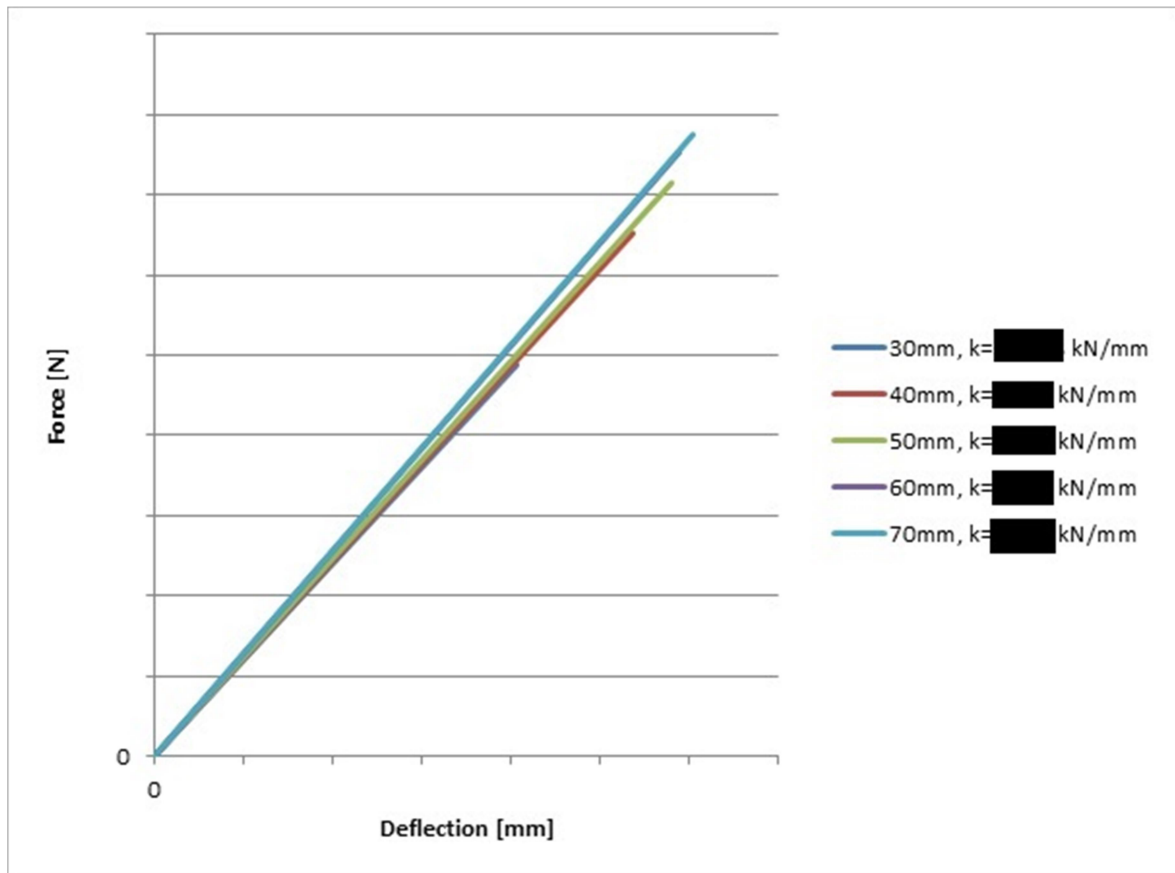


Figure 5.16 Dimensions of different connection fittings

### 5.3.2. Results

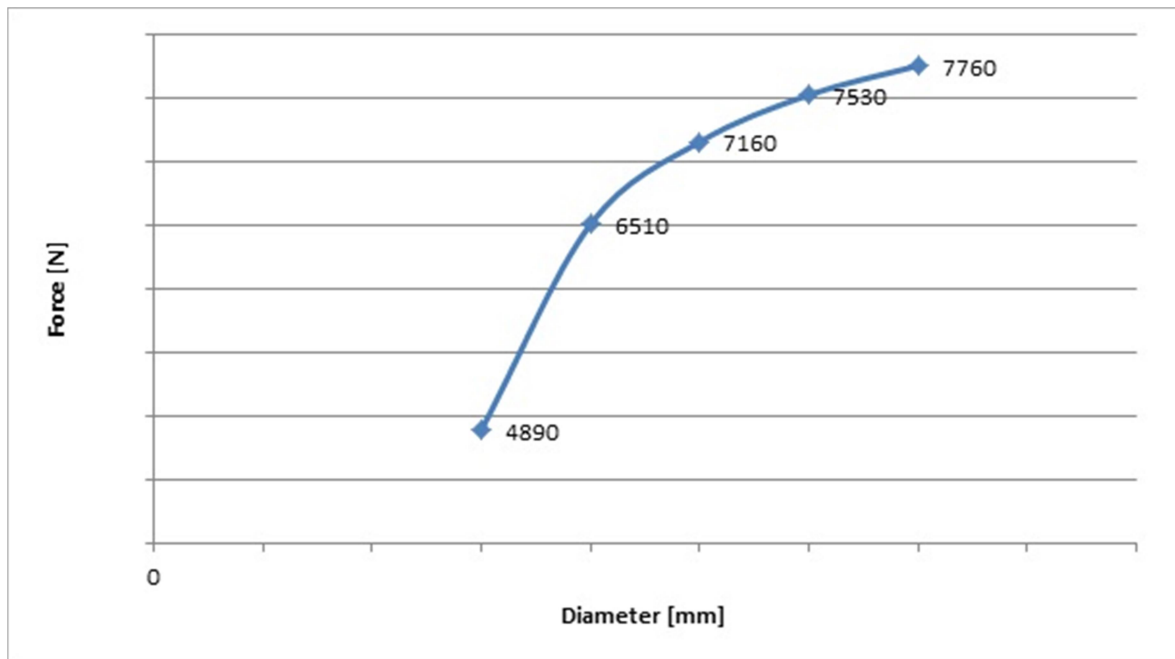
The stiffness of the blind point connection is nearly the same for every model thus not depending on the diameter of the contact area. The value of stiffness ranges from [redacted] kN/mm to [redacted] kN/mm (graph 9).



Graph 9 Stiffnesses of different connection fittings

The delamination force however changes significantly. The graph 10 shows the dependency of the diameter of the contact area on the delamination force value. There is clearly huge delamination resistance difference between connection fitting with diameter of 30 mm and one with diameter of 40 mm. Then the delamination force rises with slower and slower rate.

It is an opinion of the author that connection with contact area with diameters ranging from 42 mm to 45 mm (as seen in the graph 10) could perform well with little additional cost for extra material.



Graph 10 Delamination force-diameter dependency

## 6. Conclusion

The basic characteristics of the blind point connection under tensional load were presented. Three experiments were performed and a numerical model was created reflecting the results of those experiments. Material characteristics were used as presented in tables 3, 4, 5 and 6. The material characteristics of SentryGlass foil were modified the most since their typical values provided by the producer do not correspond with test results of performed experiments. The work was performed in such way that the visco-elastic behavior of the interlayer foil could be omitted (short-term loading, constant temperature).

The behavior of such connection is linear until delamination of the connection fitting. There is a sudden increase of deformation of approximately      mm after the delamination. The stiffness of such delaminated connection slightly drops but the behavior remains linear until the delamination occurs also between the glass and the interlayer foil, the laminated unit loses its composite behavior and fails.

However there were only three experiments performed thus there is not enough data for statistical evaluation the author suggests following regulations for blind point connections under tensional loading:

- The service limit state load of such connection should be set in such way that there is never reached the connection fitting delamination (from the performed experiments:  $F_{delam,k} = \blacksquare$  kN)
- The ultimate limit state of such connection should reflect the ability to maintain residual load-bearing capacity even after the connection fitting delamination. The data from the experiment suggest that in our case it would be  $F_{Rk} = \blacksquare$  kN

It must be noted that the real characteristic values for SLS and ULS should be obtained statistically as a result of larger scale experiments. The values presented here are only for illustration of a problem.

## 6.1. Summary

The scheme of the performed work can be seen in figure 6.1.

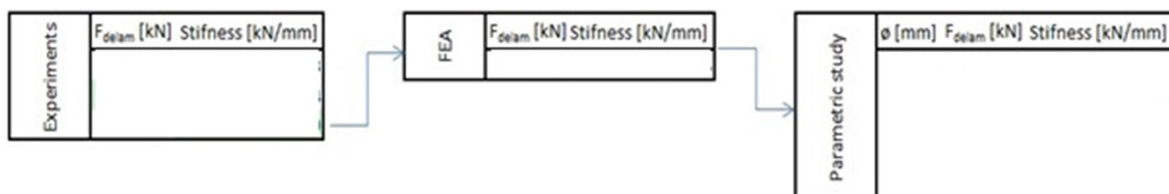


Figure 6.1 Scheme of the performed work

The conclusions from the presented work are:

- The blind point connection is a very well made design although the prediction of its behavior is very complicated
- The delamination occurs as an initial failure but there is still big residual resistance after it
- The total failure occurs due to loss of the composite behavior of the laminated glass pane caused by delamination propagation

- The behavior of such connection has a linear nature both pre- and post-delamination
- The stiffness of the blind point connections is not dependent on the size of the contact area
- The contact stress needed for delamination is approximately  $\sigma_c$  MPa
- Size of the contact area strongly influences the value of force needed for delamination

## 6.2.Future extensions

The work on this subject could be carried on by addressing following issues:

- Provide experiments on larger number of samples to obtain data needed for identifying the characteristic values of load needed for delamination and total failure
- Introduce the visco-elastic behavior of the interlayer foil into the numerical model
- Providing data needed for introduction of Fracture-Energies based Debonding to the numerical model as it appears to be the ideal cohesive zone modeling alternative
- Provide experiments and a numerical model of the blind point connection subjected to bending moments
- Provide experiments and a numerical model of the blind point connection subjected to load combination of bending moments and tensional force
- Provide a numerical model describing the post-delamination behavior and total failure of the laminated glass pane
- Perform a parametric study with different input parameters (for example angle of the conic part of the connection fitting)

## 7. Bibliography

1. WURM, Jan. *Glass structures: design and construction of self-supporting skins*. Basel: Birkhäuser, c2007. ISBN 978-3-7643-7607-9.
2. WALD, František, Josef MACHÁČEK, Martina ELIÁŠOVÁ, et al. *Novinky v navrhování ocelových a dřevěných konstrukcí se zaměřením na skleněné konstrukce*. Praha: České vysoké učení technické v Praze, 2015. ISBN 978-80-01-05780-3.
3. FELDMANN, Markus, DIMOVA, Silvia (ed.). *Guidance for European structural design of glass components: support to the implementation, harmonization and further development of the Eurocodes*. Luxembourg: Publications Office for the European Union, 2014. EUR. ISBN 978-92-79-35094-8.
4. NESTEROVA, Mariia. (2016). *Determination of material properties of viscoelastic interlayers for laminated glasses*. Master's thesis.
5. ZEMANOVÁ, Alena. (2014). *Numerical modeling of laminated glass structures*. Ph.D. Thesis.
6. VENCL, Radim. (2011). *Analýza chování nepředepnutých šroubovaných spojů konstrukcí ze skla*. Ph.D. Thesis.
7. HOŘKÝ, Radek. (2013). *Statická analýza stavebních prvků ze skla*. Master's thesis.
8. AKTER, Shaheda Tahmina, KHANI, Mohammad Sadegh. (2013). *Characterisation of laminated glass for structural applications*. Master's thesis.
9. PANAIT, Adrian, HE, Qi-Chang, MORCANT, Karine, COSSAVELLA, Michel, 2005. *Friction-grip Bolted Connections for Structural Glass Elements: Practical Solutions Using an Experimental and Numerical Coupled Approach*. *Glass Processing Days 2005*.
10. ELIÁŠOVÁ, Martina. *Lectures of Glass structures*, Department of Steel and Timber Structures, Faculty of Civil Engineering, CTU in Prague. 2015.
11. Tangram Technologies LTD. *Float Glass Production*. [www.tangram.co.uk](http://www.tangram.co.uk) [online]. ©2004 [accessed on 2016-11-09]. Available at: <http://www.tangram.co.uk/TI-Glazing-Float%20Glass.html>
12. KOZŁOWSKI, Marcin. *Hybrid Glass Beams: Review of Research Projects and Applications*. *Architecture Civil Engineering Environment* [online]. **2012**(3), 53 - 62 [accessed on 2016-11-10]. Available at:

[https://www.google.cz/url?sa=t&rct=j&q=&esrc=s&source=web&cd=1&ved=0ahUKewi0y7Hq7p3QAhVoL8AKHQKRD88QFggfMAA&url=http%3A%2F%2Facee-journal.pl%2Fcmd.php%3Fcmd%3Ddownload%26id%3Ddbitem%3Aarticle%3Aid%3D244%26field%3Dfullpdf&usg=AFQjCNHmp\\_BcoSZ7rME0PpNjJHJFnQJCmQ&sig2=eoVN-6c1ZLsUBrtjqrXBg&bvm=bv.138169073,d.ZGg&cad=rja](https://www.google.cz/url?sa=t&rct=j&q=&esrc=s&source=web&cd=1&ved=0ahUKewi0y7Hq7p3QAhVoL8AKHQKRD88QFggfMAA&url=http%3A%2F%2Facee-journal.pl%2Fcmd.php%3Fcmd%3Ddownload%26id%3Ddbitem%3Aarticle%3Aid%3D244%26field%3Dfullpdf&usg=AFQjCNHmp_BcoSZ7rME0PpNjJHJFnQJCmQ&sig2=eoVN-6c1ZLsUBrtjqrXBg&bvm=bv.138169073,d.ZGg&cad=rja)

13. DRAFT prEN 16612. Glass in building - Determination of the load resistance of glass panes by calculation and testing. 2013
14. DRAFT prEN 16613. Glass in building - Laminated glass and laminated safety glass - Determination of interlayer mechanical properties. 2013
15. ANSYS Workbench 16.2 documentation
16. Kuararay Europe GmbH. [www.trosifol.com](http://www.trosifol.com) [online]. [accessed on 2.12.2016].

Available at:

[http://www.trosifol.com/fileadmin/user\\_upload/TROSIFOL/support/downloads/technical\\_information/150129\\_Kuraray\\_TM\\_Datenblatt\\_SG.pdf](http://www.trosifol.com/fileadmin/user_upload/TROSIFOL/support/downloads/technical_information/150129_Kuraray_TM_Datenblatt_SG.pdf)